Universidade de Aveiro
Ano 2015

Departamento de Engenharia de Materiais e Cerâmica

Carina Guedes da Costa

Control of cathodic reactivity via active protective layers

Airbus Group Innovations

Metallic Technologies & Surface Engineering

Universidade de Aveiro
Ano 2015

Departamento de Engenharia de Materiais e Cerâmica

Carina Guedes da Costa

Control of cathodic reactivity via active protective layers

Dissertation submitted to the University of Aveiro to fulfil the requirements for obtaining a Master's degree in materials engineering, held under the scientific guidance of Dr. Mikhail Zhelukedvich invited associate professor in the Department of Ceramic and Materials Engineering at the University of Aveiro and supervision of Senior expert Theo Hack and Sonja Nixon from Airbus Group.

Airbus Group Innovations

Metallic Technologies & Surface Engineering

The jury

president

Doctor João Tedim

Research Assistant in the Departament Materials and Ceramic Engineering

Associate professor Mikhail Zheludkevich

Associate professor in Department of Materials and Ceramic Engineering at the University of Aveiro

Doctor Frederico Calheiros Maia

R&D Director of Smallmatek

Acknowledgements

I would like to express my sincere gratitude to my research advisor Dr. Mikhail Zheludkevich for all the support during my thesis. I address many thanks to my supervisors Theo Hack and Sonja Nixon at Airbus Group Innovation for their help with experimental work and guidance and for giving me this amazing opportunity to work in an industrial environment.

Special and measureless thanks to my family and to my best friend Ana Rita Fernando for all the moral support and patience during my academic path and in particular the last year.

I am particularly thankful to my friends Ana Caetano, Jorge Carneiro, Dr. João Tedim, Dr. Cristina Neves, Dr. Isabel Sousa and Frederico Maia for all their knowledge, wisdom, advice, support and friendship.

Many thanks to my colleagues and friends at Airbus Adrien Murillon, Steffen Reichel, Philipp Strobach, Tobias Strobl, Jakob Wissner, Luigi Aloe and Tiago Von Hafe for all the good times provided in- and outside the company and for all the incalculable support without them would have been more difficult.

Lastly, I would like to thank to my flatmates and friends Olga Devive, Norbert Karpen, Daniela Becker, Jasper Clemens, Chris Marbaise and Kai Sanwald for the amazing moments that we spent together, for listening and sharing ideas in this final stage of my thesis.

Resumo

O presente trabalho encontra-se dividido em quatro subtópicos: (1) Design do suporte para as amostras, (2) a escolha do inibidor e do tipo de revestimentos, (3) a incorporação dos nanocontentores nos revestimentos e por fim (4) a avaliação da eficiência dos sistemas criados.

O suporte das amostras acopladas foi concebido tendo em conta o efeito galvânico entre as duas amostras. Os revestimentos a utilizar foram escolhidos epóxi e sol-gel A principal função destes revestimentos ´inteligentes´ é proteger liga de aluminio 2024 da corrosão, quando está acoplada galvanicamente com o polímero reforçado com fibras de carbono (CFRP). Em cada revestimento foram incorporados dois tipos de nanocontentores, LDH Mg/Al e Bentonite, carregados com o respectivo inibidor. Os nanocontentores LDH foram carregados com um inibidor orgânico 1,2,3-benzotriazole. No caso dos nanocontentores de bentonite o inibidor incorporado foi $Ce(NO)_3$.

A incorporação dos nanocontentores foi realizada por via mecânica por forma a obter uma maior homogeneidade. A liga de aluminio foi submetida a um pré – tratamento (Socosurf) e o polímero reforçado com fibras de carbono foi aplicado um pré-tratamento de Plasma pressão atmosférica.

Por forma a avaliar a eficiência e propriedades anticorrosivas quer dos revestimentos quer dos inibidores, foram utilizadas as técnicas de caracterização: espectroscopia de impedância electroquímica (EIS), microscopia ótica, testes de adesão e teste de nevoeiro salino (SST).

O trabalho foi realizado em ambiente industrial (Airbus Group Innovations).

Palavras-chave Revestimentos inteligentes, inibidores , sol-gel, protecção contra corrosão, Plasma, CFRP, nanocontentores.

Abstract

This work is divided into four sub-topics: (1) Design support for the samples; (2) the choice of the inhibitor and the type of coating, (3) the incorporation of nanocontainers in coatings and lastly (4) the efficiency of the chosen systems.

The support of the coupled samples was designed to prove the galvanic effect between the two samples. Taking into account, the coatings were chosen using epoxy and sol-gel, the function of these "smart" coatings is to protect aluminum 2024 alloy, when electrically coupled to carbon fiber reinforced plastic (CFRP), against corrosion. In each coating two types of nanocontainers were incorporated, LDH Mg / Al and Bentonite, loaded with the respective inhibitor. The LDH nanocontainers were loaded with an organic inhibitor 1,2,3-benzotriazole. In the case of Bentonite nanocontainers the embedded inhibitor was Ce $(NO)_3$.

The incorporation of nanocontainers was accomplished through mechanical stirring in order to achieve greater uniformity. On the aluminum alloy and on the carbon fiber reinforced plastic a pre-treatment (Socosurf) and a pre-treatment Atmospheric Pressure Plasma, respectively were applied. In order to test the efficiency and anticorrosive properties of the coating and inhibitors, electrochemical impedance spectroscopy (EIS), optical microscopy, adhesion test and salt spray test (SST) were used.

The work was carried out in an industrial environment (Airbus Group Innovations).

Key-words

Smart coatings, inhibitors, sol-gel, corrosion protection, Plasma treatment, CFRP.

Abstrakt

Diese Arbeit ist in vier Unterthemen unterteilt: (1) Design-Unterstützung für die Proben; (2) die Auswahl des Inhibitors und die Art der Beschichtung, (3) der Einbau von Nanocontainern in Beschichtungen und schließlich (4) der Wirkungsgrad der ausgewählten Systeme.

Der Träger der verbundenen Proben wurde entwickelt, um die galvanische Wirkung zwischen den beiden Proben nachzuweisen. Unter Berücksichtigung, dass die Beschichtungen unter Verwendung von Epoxidharz und Sol-Gel gewählt wurden, ist die Funktion dieser "smart coatings" der Schutz gegen Korrosion von Aluminium 2024-Legierung, wenn diese elektrisch mit Kohlefaserverstärktem Kunststoff (CFK) gekoppelt wird. In jeder Beschichtung wurden zwei Arten von Nanocontainern eingebracht, LDH Mg / Al und Bentonit, geladen mit dem jeweiligen Inhibitor. Die Nanocontainer LDH wurden mit einem organischen Inhibitor 1,2,3-Benzotriazol geladen. Im Falle der Bentonit Nanocontainer war der eingebettete Inhibitor Ce $(NO)_3$.

Der Einbau von Nanocontainern wurde durch mechanisches Rühren verwirklicht, um eine größere Homogenität zu erreichen. Auf die Aluminiumlegierung wurde eine Socosurf-Vorbehandlung angewendet und auf den kohlefaserverstärkten Kunststoff eine Atmosphärendruckplasma-Vorbehandlung.

Um den Wirkungsgrad und die Korrosionsschutzeigenschaften der Beschichtung und Inhibitoren zu testen, wurden elektrochemische Impedanzspektroskopie (EIS), optische Mikroskopie, Klebversuche und Salzsprühtests (SST) verwendet.

Die Arbeiten wurden in einer industriellen Umgebung durchgeführt. (Airbus-Gruppe Innovations)

Schlüsselworte Smart Coatings, Inhibitoren, Sol-Gel, Korrosionsschutz, Plasmabehandlung, CFK.

Content

Figure content

Table content

List of Abbreviations and symbols

CFRP – Carbon Fibre Reinforced Plastic

GFRP – Glass Fibre Reinforced Plastic

GC – Galvanic Corrosion

AA2024 – Aluminium Alloy 2024

BTA – 1, 2, 3-benzotriazole

$CeNO_3$ – Cerium Nitrate

LDH – Layered Double Hydroxides

AcAc – Acetylacetone

TPOT – Titanium-isopropoxide

GPTMS – 3-glycidoxypropyl trimethoxisilane

PTMS - Phenyltrimethoxysilane

APP - Atmospheric Pressure Plasma

EIS – Electrochemical Impedance Spectroscopy

XPS – X-Ray Photoelectron Spectroscopy

SEM – Scanning Electron Microscopy

ZRA – Zero Resistance Ammeter

SST – Salt Spray Test

Chapter 1: Introduction and State-of-art

1. Introduction

1.1. Motivation

Based on the growth achieved in 2014 in the commercial aerospace sector, these companies are likely to re-achieve the frame incomes and profits in the near future.
It is expected, that this will be managed primarily by the accelerated replacement cycle of old aircraft with next generation fuel-efficient aircraft, as well as the continued increase in passenger travel demand, particularly in the Middle East and the Asian Pacific regions [1]. Air travel plays an important part in the demand for aircraft and innovative aircraft technology. Consequently, the materials selection and manufacturing process continues to upgrade, with improvements powered by dramatic innovations in fuel efficiency [1,2].
The recovery of the global economy has stimulated the search for oil all around the world, increasing the pressure on energy prices. In order to fight against the significant amount of energy consumed by the aircraft equipment, the aerospace industry has to appeal to composites.
The aerospace industry claims a lot from the materials. Demands include improved toughness, lower weight, increased resistance to fatigue and corrosion. The boundaries of material properties are being constantly extended as manufactures strive to give the next generation of aircraft improved performance while making them more efficient. Aluminium alloy is one of the key materials facing these challenges.
The solution found to solve this issue was to introduce CFRP in the aircraft structure due to its low specific weight of 1.55 g/cm^3 (aluminium = 2.8 g/cm^3). Over the time it was possible to notice the presence of corrosion due to the galvanic effect between the two materials, so the solution found was to add a glass layer to isolate and prevent the galvanic corrosion. Although the isolation was efficient, this layer adds too much weight to the aircraft.

Lightweight materials are becoming increasingly important in many industries. There are three industries where lightweight has played an important role in product design: aviation, wind energy, and automotive. Figure 1 shows, that the use of aluminium alloys, in aviation, is decreasing while the use of carbon fibre is increasing [3].

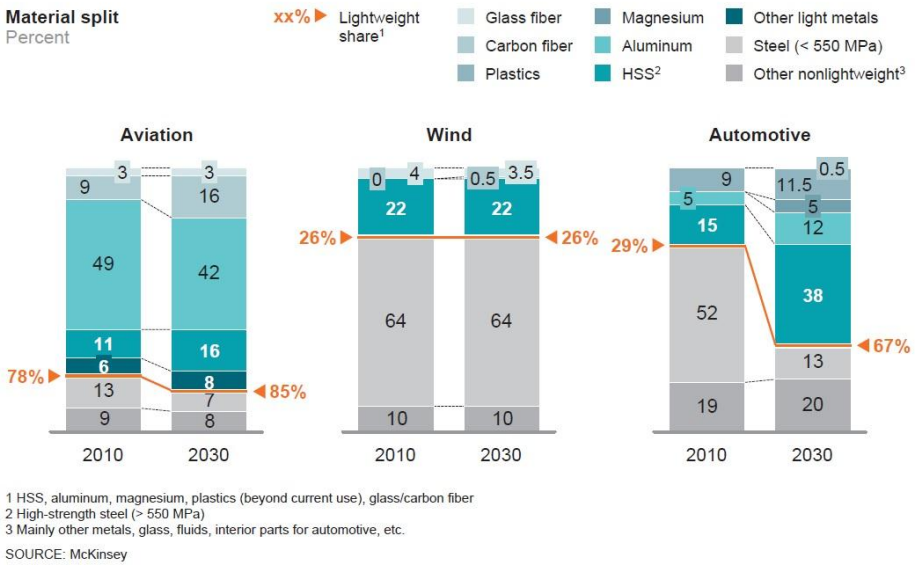

Figure 1.The most lightweight materials in terms of share [3]

In aviation, lightweight materials (such as light metals, aluminium, plastics and composites) already make up roughly 80 percent of all materials. These kinds of materials have two main drivers in aircraft industries: the need to reduce fuel consumption and related costs and the wish to increase passenger/cargo load per flight [3] Aluminium alloy is currently the most lightweight material in aviation with about 50 percent of the structural weight. However, in the new aircraft models carbon fibre already achieves 50 percent of the structural weight and therefore substitutes aluminium alloy.

Composite materials have the ability to play a distinguished role in the aircraft industry today and in the future. The main reasons why composite materials are so interesting for the aviation and aerospace applications are their remarkable durability and stiffness properties. These kinds of materials are normally composed by strong and stiff fibres in a hard matrix. In aerospace industry there are two kinds

of materials that are very often used: carbon- and glass- fibre-reinforced plastic (CFRP and GFRP, respectively).

The use of composite materials is profitable for aircraft industry because this type of material helps to reduce the overall weight of the airframe allowing higher fuel efficiency. With these materials the industry should be able to save 20% in terms of weight along with reduction of production time and an upgrading of damage tolerance.

For example, the Airbus A380 was built with 20% to 22% of composites combined with Glass-fibre-reinforced aluminium alloy (GLARE) [2].

Being a lightweight material is one of the most important advantages of carbon fibres, but on top this material offers a number of advantages such as corrosion resistance, non-magnetic properties, high tensile strength and ease of handling. However, carbon fibre reinforced has a linear elastic response in tension up to failure and a poor transverse or shear resistance. It also has a poor resistance to fire and high temperatures. This type of material loses strength upon bending and it is sensitive to stress-rupture effects [4].

Taking these properties into account, the use of hybrid materials (metal with composites) will be an interesting subject for the future.

Recently the aircraft design has focused on the most ordinary aluminium alloy 2024. This alloy can induce galvanic corrosion when coupled with CFRP due to the electrochemical behaviour of carbon fibres [5]. Taking into account the problems listed before, the purpose for this master thesis is to focus on finding new ways to prevent galvanic corrosion avoiding the chromate-containing paints and the glass layer.

For this work two different formulations of coatings were used, sol-gel coating and epoxy coating. Nanocontainers, such as LDH and Bentonite carrying inhibitors, were added into the coatings in order to increase their protective properties.

1.2. Thesis structure

This master thesis it is divided into sections as follows:

- **State-of the-art:** brief explanation of the topic.
- **Literature Review:**
  - Galvanic Corrosion
  - Corrosion Protection: types of inhibitors, encapsulation technologies and active protective coatings
  - Sol-gel formulation
- **Assembly Design**
- **Materials and Methods:**
  - Sol-gel Synthesis
  - Plasma treatment
  - Analytical methods and apparatus: description of all the techniques used during this thesis
- **Experimental**
- **Results and Discussion**
- **Conclusion**

Chapter 2: Theorycal Background

2. Theoretical Background

2.1. Corrosion

Corrosion manifests itself in multifarious forms in our daily lives, corroded automobiles, nails, pipes, pots, pans or shovels. Metallic corrosion has been a problem since ordinary metals were first put into use [6,7]. Corrosion, when mentioned in this thesis, refers to the electrochemical corrosion of metals.

Most metals naturally occur as compounds, such as oxides, sulfites, silicates, or carbonates. Very few metals occur in native form. The obvious reason is the thermodynamic stability of compounds as opposed to the metals [6]. Any corrosion reaction in aqueous solution must involve oxidation (anodic reaction) of the metal and reduction (cathodic reaction) of a species in solution, in consequence electrons transfer between the two reactants. The anodic and cathodic reactions occur at the same rate and simultaneously upon a metal's surface, therefore the metal is electrically charged, and thus the rate of oxidation is equal to the rate of reduction.

For example in this situation, the corrosion of aluminium in water can be represented by two half reactions:

Oxidation(anodic reaction)	$Al \rightarrow Al^{3+} + 3e^-$	(1)
Reduction(cathodic reaction)	$2H_2O + 2e^- \rightarrow H_2 + 2OH^-$ $2H_2O + O_2 + 4e^- \rightarrow 4OH^-$	(2)

Corrosion is a problem extremely expensive and serious for materials science [6].

2.1.1. Galvanic Corrosion

Corrosion can be defined as the degradation of material due to a reaction with its environment. This degradation implies deterioration of physical properties of the material. The forms of corrosion have been identified based on the apparent morphology of corrosion, the basic factor influencing the mechanism of corrosion in each form [7]. Corrosion can manifest in many forms, such as uniform or general corrosion, galvanic corrosion, crevice corrosion, pitting corrosion, intergranular

corrosion, selective leaching, erosion corrosion, stress corrosion, corrosion fatigue and fretting corrosion.

This thesis will focus on the galvanic corrosion, so a more detailed description will be discussed in the following paragraphs.

Nature has endowed each metallic substance with a certain natural energy level or potential. When two metals, having different energy levels or potentials, are coupled together, current will flow. Corrosion will occur at the point where positive current leaves the metal surface [8].

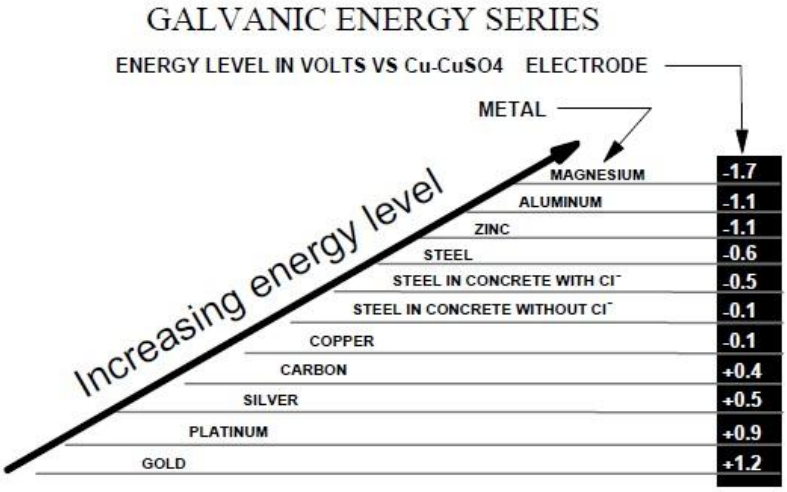

Figure 2.Galvanic use energy series [8].

Galvanic Corrosion (GC) is, at first, characterized through the localization of the main processes anodic and cathodic in distinct regions. These different spots can be seen on the metal surface between different microscopic phases, but also between two distinct materials with different electrochemical properties that are coupled in the presence of a corrosive electrolyte. Therefore, galvanic corrosion is the unwelcome result of this hybrid materials usage and the severity of attack decreases with increasing distance from the junction. This distance affected depends upon the conductivity of the solution [5,8,9].

This electrochemical process between the two dissimilar materials depends on the Gibbs free energy, ΔG:

$$\Delta(\Delta G) = - \Delta E.n.F \qquad (3)$$

n = Number of electrons taking place in the reaction

ΔE =EMF (difference between the EMFs (electromotive force) of the two materials of the corrosion couple)

F = Faraday's constant

The main phases in the operation of a galvanic corrosion cell are illustrated in Figure 3, in chloride ions containing electrolyte which are the most relevant ones in-service. The less noble metal acts as the anode and is oxidized according to:

$$M \rightarrow M^{n+} + ne^- \quad (4)$$

The cathodic process in GC in near –neutral electrolyte is commonly stated in terms of the oxygen reduction reaction:

$$O_2 + 2H_2O + 4e^- \rightarrow 4OH^- \quad (5)$$

In this electrochemical system, the current flow between anode and cathode either between two different materials or on a single material will take place by the displacement of electrons from anodic to cathodic regions and in the solution by the movement of cations from anodic to cathodic regions and movement of anions in the opposite direction. The effect of galvanic corrosion into the material will thus appear mainly on the anodes. In the case of CFRP, it behaves as an inert material, no material dissolution has to be expected. This type of corrosion can occur on two levels: macroscopic and microscopic [5].

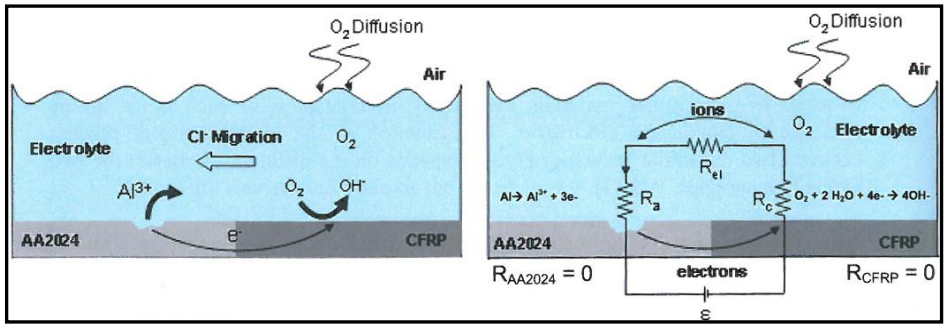

Figure 3.Scheme of a galvanic corrosion macroscopic cell a) AA2024 coupled with CFRP; b) circuit model for direct 4 electrons oxygen reduction step [5].

Regarding Figure 3b) the galvanic corrosion current can be expressed:

$$I_{gal} = \frac{\varepsilon}{R_a + R_c + R_{el} + R_{AA2024} + R_{CFRP}} \quad (6)$$

With:

I_{gal} :	Corrosion current	[A]
ε :	Potential difference between uncoupled anode and cathode	[V]
R_a :	Polarization resistance of anode	[Ω]
R_c :	Polarization resistance of the cathode	[Ω]
R_{el} :	Electrolyte resistance between anode and cathode	[Ω]
R_{AA2024} :	AA2024 electrode resistance = 0 (assuming aluminium as perfect conductor)	
R_{CFRP} :	CFRP electrode resistance = 0 (assuming all carbon fibres are well connected)	

R_{CFRP} and R_{AA2024} are considered to be zero. Due to the fact that they are nearly insignificant in value due to direct electrical contact compared with other resistances. During this procedure one of the resistances becomes extremely high, for example when they are in the presence of a coating system it's not possible on any of the electrodes to observe any significant corrosion rates due to the galvanic effects except for self-corrosion of AA2024 [5].

New aircraft designs contain a high degree of CFRP materials which are in contact with aluminium in specific areas. Galvanic Corrosion can be induced, since the carbon fibres behave electrochemically like a noble metal where cathodic corrosion reaction will take place and the aluminium alloy is preferentially corroded [9].

2.2. **Corrosion Protection**

Distinct prevention methods exist to decrease the corrosion process. The most advancing protective methods are directly associated to the definition of corrosion. One can either change (1) the type of material, change the way they (2) interact or change the (3) environment.

(1) The selection of the metal itself will be the first step in corrosion prevention management. Depending on the environment, different metals will corrode more

easily: The binding of corrosion thermodynamics between metal and pH can be clearly plotted in Poourbaix diagrams. Iron will oxidize at pH 7 and it holds a surface potential above -0.7 V (vs SHE). The resultant hydroxide is soluble in water and corrosion will take place. Aluminium as well will oxidize but the formed products are insoluble and a passivating oxide layer will be created under these conditions, thus protecting the surface from corroding.

(2) The corrosion process can be diminished through the formation of a barrier at the metal solution interface. Applying a coating to a substrate is a very common approach in order to obtain a separation of metal and environment. This barrier layer can be an organic, inorganic or metallic layer. However, often combinations of different coatings are used to make multifunctional systems with synergistic protective effect.

(3) Changing the environment to limit the corrosion process can also be an approach. For example this can be achieved by adding inhibitors to a cooling water stream or by changing the pH to obtain a less corroding environment. An adjustment in pH can cause a shift in solubility of the corrosion products causing a protective film to be formed on the metal surface.

Corrosion inhibition corresponds to the addition of chemicals known as corrosion inhibitors, which minimize the rate of corrosion. Corrosion inhibitors modify electrochemical reactions by their action from the solution side of the metal /solution interface, and the increase in corrosion resistance can be measured by various parameters [7,10].

Corrosion inhibitors are used in multiple industrial applications, including potable water, cooling water systems, automobile engine coolants, acid pickling solutions, to protect reinforcing steel bars in concrete, and in oil recovery and storage.

Inhibitors are also used in the surface treatment of metals to improve the corrosion resistance (chromates on aluminium alloys or galvanized steel) or to improve their paint adhesion (phosphates on auto body steel sheets). Corrosion inhibitors can also be incorporated into paints or organic coatings [10].

The corrosion inhibitors can be either synthetic or natural chemicals and can be classified by: the chemical nature as organic or inorganic; the mechanism of action as

anodic, cathodic or anodic-cathodic mix and by adsorption action, or; as oxidants or not oxidants.

This chapter will be divided according to the classification of the inhibitors shown in Figure 4.

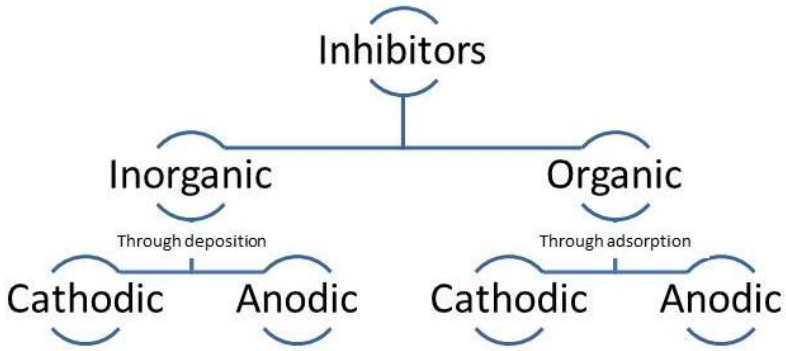

Figure 4. Inhibitors classification.

2.2.1. Inorganic inhibitors

2.2.1.1. Anodic inhibitors

Anodic inhibitors, also known as passivation inhibitors, act by a reducing anodic reaction which means, that they block the anode reaction and support the natural reaction of passivation metal surface. Also because the formation of a film adsorbed on the metal occurs. In general, the inhibitors react with the corrosion product, initially formed, resulting in a cohesive and insoluble film on the metal surface. Figure 5 shows a potentiostatic polarization diagram of a solution with behaviour of anodic inhibitors. The anodic reaction is affected by the corrosion inhibitors and the corrosion potential of the metal is shifted to more positive values. The presence of corrosion inhibitors also affects the value of the current decrease.

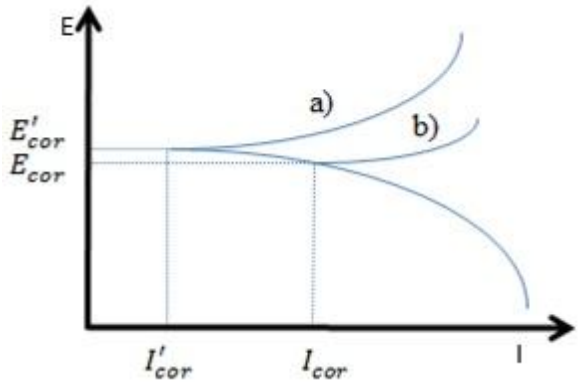

Figure 5.Potentiostatic polarization diagram: electrochemical behaviour of a metal in a solution with anodic inhibitor (a) versus without inhibitor (b) [11].

When the concentration of inhibitors becomes high enough, the cathodic current density at the primary passivation potential becomes higher than the critical anodic current density, shifting the potential for a noble sense and, consequently, passivating the metal. For the anodic inhibitors effect, it is very important that the inhibitor concentrations should be high enough in the solution. The inappropriate amount of inhibitors affects the formation of film protection, because it will not cover the metal completely, leaving sites of the metal exposed, thus causing a localized corrosion.
Some examples of inorganic anodic inhibitors are nitrates, molybdates, sodium chromates, phosphates, hydroxides and silicates.

2.2.1.2. Cathodic inhibitors

During the corrosion process, the cathodic corrosion inhibitors prevent the occurrence of the cathodic reaction of the metal. Depositting a compact and adherent film over the metal, the diffusion of reducible species in these areas get restricted. These inhibitors cause high cathodic inhibition. Figure 6 shows an example of a polarization curve of the metal on the solution with a cathodic inhibitor. When the cathodic reaction is affected, the corrosion potential is shifted to more negative values.

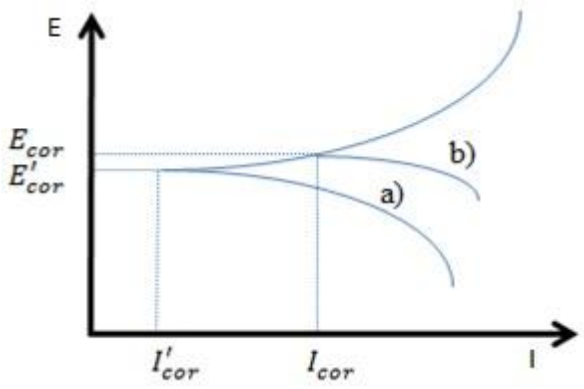

Figure 6. Potentiostatic polarization diagram: electrochemical behaviour of the metal in a cathodic inhibitors solution (a), as compared to the same solution, without inhibitor (b) [11].

The cathodic inhibitors form a barrier of insoluble precipitates over the metal, covering it. Thus, it restricts the metal contact with the environment, even if it is completely immersed, preventing the occurrence of the corrosion reaction. In consequence, the cathodic inhibitor is independent of concentration, thus, they are considerably more secure than anodic inhibitor. Figure 7 shows the illustration of the mechanical effect of cathodic inhibitors to restrain the corrosion process.

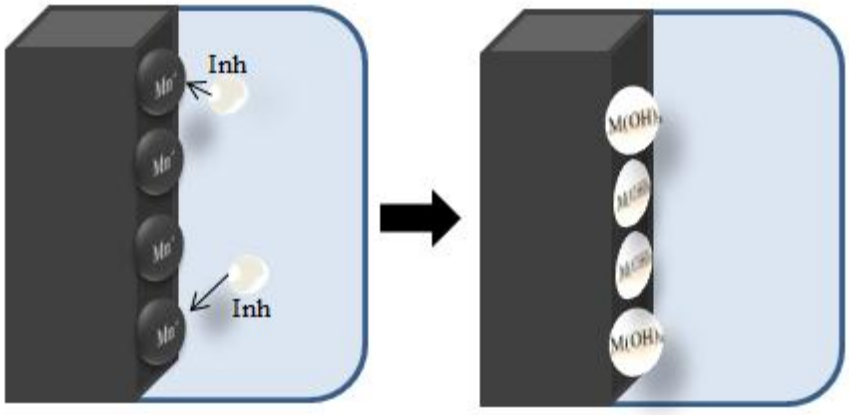

Figure 7. Cathodic inhibitors effect and their mechanism [11].

Some examples of inorganic cathodic inhibitors are the ions of the magnesium, zinc, and nickel that react with the hydroxide anian (OH^-) of the water forming the insoluble hydroxides as ($Mg(OH)_2$, $Zn(OH)_2$, $Ni(OH)_2$), which are deposited on the cathodic site of the metal surface, protecting it. Polyphosphates, phosphonates, tannins, lignins and calcium salts are further examples presenting the same reaction mechanism.

2.2.2. Organic inhibitors

Organic compounds used as inhibitors occasionally act as cathodic, anodic or both, as cathodic and anodic inhibitors. Nevertheless, as a general rule, they act through a process of surface adsorption, nominated as a film- forming. Naturally the occurrence of molecules exhibiting a strong affinity for metal surfaces compounds showing good inhibition efficiency and low environmental risk. These inhibitors build up a protective film of adsorbed molecules on the metal surface, which provides a barrier to the dissolution of the metal in the electrolyte. They must be soluble or dispersible in the medium surrounding the metal. In Figure 8, showing a theoric potentiostatic polarization curve, it can be seen that the effect of the solution containing organic inhibitor on the metal presents an anodic and cathodic behaviour. After the addition of the inhibitor, the corrosion potential remains the same, but the current decreases from I_{cor} to I'_{cor}.

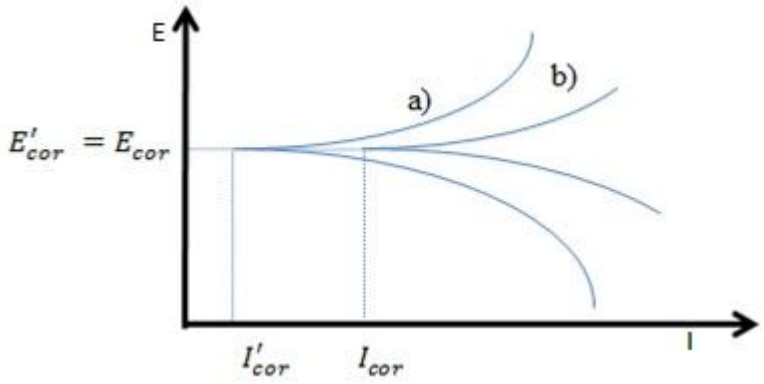

Figure 8. Theoretical potentiostatic polarization diagram: electrochemical behaviour a metal on a solution containing a cathodic and anodic inhibitor (a) compared to the same solution without the inhibitor (b) [11].

In Figure 9 the mechanism of actuation of organic inhibitors is shown, when it is adsorbed to the metal surface and forms a protector film on it.

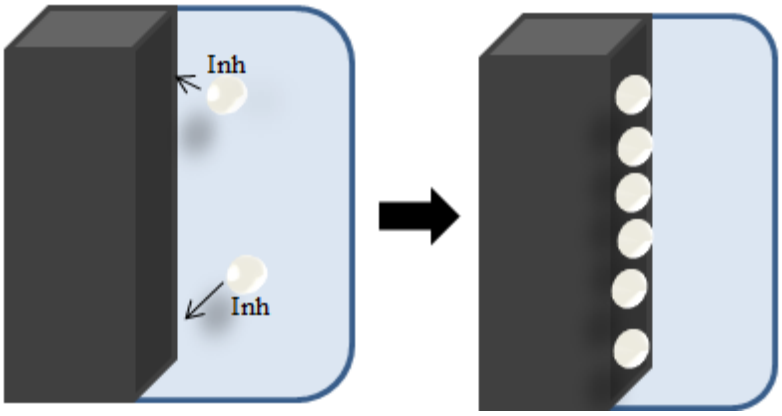

Figure 9. Illustration of the mechanism of actuation of the organic inhibitor: acting through adsorption of the inhibitor on the metal surface. Inh represents the inhibitor molecules [11].

The efficiency of an organic inhibitor depends of the:

- chemical structure, like the size of the organic molecule;
- aromaticity and/or conjugated bonding, as the carbon chain length;
- type and number of bonding atoms or groups in the molecule (either π or σ);
- nature and the charges of the metal surface of adsorption mode like bonding strength to metal substrate;
- ability of a layer to become compact or cross-linked,
- capability to form a complex with the atom as a solid within the metal lattice;
- type of the electrolyte solution like adequate solubility in the environment.

The efficiency of these organic corrosion inhibitors is related to the presence of polar functional groups with S, O or N atoms in the molecule. Heterocyclic compounds and pi electrons, generally have hydrophilic or hydrophobic parts ionisable. The polar function is usually viewed as the reaction centre for the establishment of the adsorption process. The organic acid inhibitor that contains oxygen, nitrogen and/or sulfur is adsorbed on the metallic surface, blocking the active corrosion sites. Although the most effective and efficient organic inhibitors are compounds that have π-bonds, it presents biological toxicity and environmentally harmful characteristics.

Some examples are amines, urea, toliotriazol, aldehydes, sulfur-containing compounds and acetylenic compounds and also ascorbic acid, succinic acid, tryptamine, caffeine and extracts of natural substances and heterocyclic nitrogen compounds for example 1, 2, 3 - benzotriazole (BTA).

2.2.3. Choice of the inhibitors

Many factors have to be considered, when choosing an inhibitor including the cost and the amount, easy availability and safety to the environment and its species. The choice of the fitting corrosion inhibitors must follow some aspects including structural and environmental considerations.

Structural aspects which belong to the performance of organic inhibitors are related to the chemical structure and physicochemical properties of the compound like functional groups, electron density at the donor atom, p-orbital character, and the electronic structure of the molecule. Structural factors which contribute to the action of inhibitors are:

(i) Chain length,

(ii) Size of the molecule,

(iii) Bonding, aromatic/conjugate,

(iv) Strength of bonding to the substrate,

(v) Cross-linking ability,

(vi) Solubility in the environment.

The choice of this set of inhibitors was based on previous works [25],where the efficiency of inhibitors was systematicly analysed. After this study it was possible to conclude, that the mixture of inhibitors (BTA combined with $CeNO_3$) was performing better than the rest, especially with the cases of galvanic corrosion.

Therefore, the inhibitors chosen for this study were 1, 2, 3-benzotriazole (BTA) and Cerium Nitrate ($CeNO_3$), in order to obtain good corrosion protection.

Several heterocyclic compounds containing nitrogen atoms have been used as effective inhibitors for copper and copper alloys in many enviroments and applications. The accelerated corrosion of copper surfaces results in a galvanic deposition of copper into existing ferrous metal surfaces, which can have detrimental effects on the structural integrity and operation of cooling system. 1, 2, 3 - benzotriazole is a heterocyclic compound containing three nitrogen atoms, this aromatic compound is colorless and polar and can be used in various fields.[26]

2.2.4. Encapsulation techniques

In order to incorporate the inhibitors mentioned above we are going to use encapsulation techniques. The embedded containers store the inhibitor and prevent any destructive interaction with the coating matrix. When the barrier properties are compromised, the inhibitor is released i.e. at coating rupture. This release is triggered by changes in the local environment in the damaged area, such as modifications in the local pH, ionic strength, humidity or the presence of aggressive ions. The inhibitor molecules either deactivate the corrosive species or form a thin protective film over the exposed metal surface. Therefore, the anticorrosive properties of the coating are recovered due to its active protection offered by the encapsulated inhibitor.

During this study the inhibitors, BTA and $CeNO_3$, will be carried by LDH and Bentonite, respectively.

According to previous studies BTA can prevent corrosion when incorporated into a nanocontainer [12]. Regarding the CeNO the addition of cerium-based inhibitiors at any hydrolysing step improves the corrosion protective properties of the coating [12].

2.2.4.1. Bentonite

Bentonite clays are a form of montmorillonite and exhibit intrinsic cation exchange properties. They are composed by negatively charged aluminosilicate layers. The negative charge of these layers is compensated by the cations intercalated between the aluminosilicate sheets. The interaction between the sheets and the exchangeable cations is purely electrostatic. Calcium (III) and cerium (III) cation-exchanged bentonite can be used as containers of respective inhibiting cations [13,14].

Cerium (III) ions are known to be effective cathodic inhibitors for AA2024 – T3. When incorporated in an anticorrosive coating for AA2024 – T3, these cerium loaded cation-exchangers have two positive functionalities: (i) they entrap cations (Al^{3+}) and (ii) release Ce^{3+} ions, which react with hydroxide ions to build insoluble cerium hydroxide precipitates on the cathodic sites. As a result of this cation exchange, corrosion activity is effectively decreased. [13]

2.2.4.2. Layered double hydroxide

Anion exchangers are promising structures for immobilization of anionic inhibitors, which can be exchanged with corrosive chloride ions. In order to achieve an effective

anion exchange, it is possible to use layered double hydroxide (LDH) which is a host structure. LDHs are positively charged bundles of mixed metal hydroxides. The stabilization of this structures is accomplished by anions and solvent molecules located between the positive layers. By absorbing adverse chlorides and the resulting release of inhibiting ions the anion exchange has a dual function.

Releasing inhibtors can also be caused by a pH change. At high pH values inhibitors get switched with hydroxide anions, at a lower pH entrapped inhibitors get released by the dissolving LDHs [15,16].

2.2.5. Active protective coatings

The aircraft industry places a high performance demand on the coatings used in aeronautical structures. High temperature variations produce dimensional changes on both structure and coating. Temperature and pressure changes can also cause condensation of water, which collects inside unpressurised or unheated areas of the structure. As altitude increases, lower pressures make residual liquid in the coating much more volatile and the less dense and less polluted atmosphere increases UV radiation. High humidity and salt concentrations in the atmosphere promote weathering and corrosion. Fluids used in the aircraft, such as aggressive phosphate ester based hydraulic fluids, can attack coatings from the surface or through the interface with the substrate.

Currently, the required adhesion, protection against corrosion and degradation, design and other specialized functions are obtained using several layers of coatings. Typical coating systems contain three individual coating layers. The first layer, a conversion coating, is the product of substrate pre-treatment. It is usually a very thin (≤10 μm) inorganic layer that provides corrosion protection and improved adhesion between the substrate and the primer. The primer, which is the second layer, consists of a pigmented organic resin matrix, typically a two component epoxy with a thickness of around 25 μm, and it is the main provider of corrosion protection. The top-coat is typically a resin with thicknesses from 50 to 200 μm, and is the main barrier against environmental influences such as extreme climates and ultra-violet rays; it also provides decoration and camouflage [17].

In this work there will be two coating systems: Sol-gel matrix and Epoxy paint. The specimens will have two layers of coating: the first one comes from the pre-treatment (Socosurf, Anodic film or Chemical Conversion Coating) and the second layer will be of sol-gel paint containing loaded nanocontainers, the same for the epoxy paint system.

2.3. Coating formulation

2.3.1. Sol-gel formulation

2.3.1.1. Fundamentals in sol-gel technology

A sol-gel process was reported for the first time in 1846 when Ebelman accidentally found that $SiCl_4$ and alcohol gelled on exposure to atmosphere. The production of sol-gel derived oxide films started in 1939. This process was developed by the Schott glass company and was studied in detail.

The sol-gel chemistry allows a variety of inorganic networks from silicon or metal alkoxide monomer precursors enabling the formation of homogeneous inorganic oxide materials with tailored properties such as hardness, optical transparency, chemical durability, and thermal resistance. The sol-gel method consists of the growth of inorganic networks through the formation of a colloidal suspension (sol) and gelation of the sol to form a network in a continuous liquid phase (gel).

Technically, the sol-gel processes is mainly based on hydrolysis and condensation reactions of metal alkoxides ($M(OR)_n$), because they easily react with water. The most usual precursors are alkoxides from silicon, zirconium, titanium, cerium and aluminium as shown in formula 7 where R displays an organic (typically alkyl) group.

$$Si(OR)_4, (Ti(OR)_4, Zr(OR)_4, Al(OR)_3 \quad (7)$$

During the hydrolysis reactions alkoxide groups (OR) are replaced by hydroxyl groups (OH). The reaction involves hydrolysis of alcohol groups due to interaction between the alkoxides groups and water.

Hydrolysis

hydrolysis

$$\equiv M - OR + \ H_2O \quad \rightleftarrows \quad \equiv M - OH + ROH \qquad (8)$$

Esterification

Condensation

alcohol condensation

$$\equiv M - OR \ + \ HO - M \equiv \quad \rightleftarrows \quad \equiv M - O - M \equiv + H_2O \qquad (9)$$

alcoholysis

or

water condensation

$$\equiv M - OH + HO - M \equiv \ \leftrightarrow \ \equiv M - O - M \equiv \ + H_2O \qquad (10)$$

hydrolysis

The properties of a sol-gel network depend on the relation between hydrolysis and condensation. The characteristics of sol-gel can be tailored by adjusting some parameters such as temperature, pH, time of reaction, concentrations of the precursors, type of catalyst and condensation, the molar ratio (R_m) between H_2O and Si, ageing time and temperature [12].

Due to the mechanical instability of the gel after the gel point, aging and drying are crucial and result in the high shrinkage of the gel. Therefore, sol-gel materials are at a higher level of interest in the area of functional coatings. A considerable number of applications is known starting from scratch resistant coatings on polymeric substrates, films showing photocatalytic or easy to clean effects, adhesion promoting layers, or as corrosion protection of metallic substrates.

One of the aspects, that contributes for an improvement of the adhesion is the chemical bonding between sol-gel films and aluminium substrates. Furthermore, sol-gel coatings, particularly the hybrid films, grant a thick barrier against electrolyte uptake. Nevertheless, the metal substrate will not be protected against corrosion for a long term because the coating by itself is not sufficient.[27]

Pathways for diffusion of corrosive species in the coating/metal interface are provided by the micro-pores, cracks and areas of low cross-link density existing in these types of coatings. [27]

These zones are the perfect spots for corrosion processes to start. The incorporation of oxide nanoparticles into the hybrid matrix can be decreased by the crack ability and porosity of the sol-gel films.[28] Once the coating is damaged, these kinds of films cannot offer an adequate protection due to the lack of self-healing properties.

The corrosion process in the defects can be suppressed by the incorporation of corrosion inhibitors into the sol-gel films. This will enhance the protective skills from the coatings. Phosphates, vanadates, borates, cerium and molybdenum compounds were found to have inhibiting action on the corrosion processes.[29,30,31]

According to the literature [29,34,35] some of the most effective and environmentally friendly corrosion inhibitors for aluminium alloys are derived from cerium salts.

Seemingly this is the outcome of depositing hydrated cerium oxide on the cathodic intermetallic particles, existing in the aluminium alloy, thus suppressing the cathodic reaction.[36]

Voevodin et al. [36] investigated the corrosion protection properties of the epoxy-zirconia sol-gel coatings, containing inihibitor ions salts such as $Ce(NO_3)_3$ among others. The sol-gel coatings doaped with this salt performed at least as good as the undoped epoxy-zirconia films.

The purpose of using nanoparticles as fillers in bulk materials and coatings is the modification of the macroscopic properties like mechanical resistance, optical features or surface features.

However, adding particles to organic-inorganic hybrid sol-gel systems can also have an influence on the chemical reactions and the network arrangement. It is possible to claim that common ceramics oxide particles obtain residual OH-groups on the particle surface, especially in aqueous systems, independently of the stabilisation method.

The particles can take part in the hydrolysis and condensation reaction during the sol-gel synthesis, depending on the accessibility of these groups, resulting in covalent bonds between the filler and the matrix. Thereby, reinforcement of sol-gel coatings by metal oxide particles increases the condensation rate of the inorganic part of the matrix.[37]

In this situation, the particles could reduce the adhesion of the layer to te substrate, decresing the amount of reactive OH-groups in the sol state, assuming that these are

crucial for the improvement of adhesion to the respective substrate. A higher level of cross-linking in the liquid followed by the formation of larger particles in the sol could cause an increase in the viscosity, which is demanding for the application processes like dip coating and spray coating.[38]

A proper surface modification of the particle can avoid an increase of viscosity. Taking into account the mechanical properties of particle filled sol-gel derived coatings, the linkage between particle and surrounding matrix is one of the most important parameters.[39]

Particularly in the context of scratch resistance of particle reinforced coatings, both concepts are followed: a strong interaction of filler and matrix increasing the hardness of the coating, and weak chemical forces supporting the flexibility of the material.

With regard to the fact, that commercially available particle dispersions are mainly steric stabilised with none-cross-linking groups on the particle surface, only weak interactions between particle and matrix are developed.

Therefore, the addition of particles reduces the hardness at lower concentrations and increases with a higher particle concentration in the system.[40,41]

The dispersion of particles in a coating could have an impact on its mechanical properties. A graduated dispersion of particles, with a higher degree of particles on the surface of the coating is reported to be effective against damage caused by scratches.[42]

2.3.2. Epoxy paint

Epoxy resins are high-performance polymers with wide area of application, which could be further expanded by modifying properties of the final material. It contains a minimum of two functional groups compounds so allows them to be converted into haard and infusible materials by the formation od networks.

These thermosetting polymers own exceptional properties, such as great thermal stability, adhesion, mechanical and electrical properties. [48, 49]

2.4. **Plasma treatment**

Today engineer polymers typically have low surface energies making them difficult to bond to. Static charges build up on patch during storage attracting dust and other contaminants interfere with the fact of bonding. Even if the surface is clean it made still not bond with certain materials. The plasma treatment has several advantages such as, increase production speed, improve quality and lower material cost.

Wegener et al. investigated the plasma effect on CFRP samples with the aim of surface activation for better adhesion. With a five-times plasma treatment the element concentration of the surface changes significantly. Whereas the carbon amount decreases from 80 to 40%, the oxygen quantity increases from 15 to 45%. Apart from that, additional elements such as nitrogen, silicium, sulfor and others differ after a plasma treatment, but do not have a crucial impact on the adhesion properties. [46]

Considering the work of Wegener et al. a plasma treatment presents a reliable option to activate the CFRP samples.

Untreated matrials have low surface energy, too low for the most of the adhesives to be effective. The plasma treatment process raises the surface energy to provide radically improved performance. This treatment helps bond the most inert surfaces such as plastics, ceramics and glass by adding favourable functional groups like hydroxyl and carbonyl groups.

It hence the interation of the adhesive surface by providing anchor sides for the coating.

A common definition for plasma is describing it as the fourth state of matter, that endures as an arrangement of ions and electrons. As a first thought we think of the three states of matter: solid, liquid and gas. For a common element, like water, these three states asre ice, water and steam. The difference between them is releated to theirs energy levels. When energy is added as heat to the ice, it melts and forms water. By adding more energy to evaporate water into hydrogen and oxygen in vapor form. If more eneygy is added to the vapor these gases become ionized. This process causes ionisation of these gases who became condutors of electricity. This gas electrically conductive and ionized is called Plasma. [19]

Plasma has higher energy than the corresponding solid, liquid and gas states due to the fact that it carries charged particles. These particles will confer to it a high electrical conductivity. This means that plasma can carry a lot of energy and is highly reactive, but it is not necessarily hot, as shown in Figure 10. [19]

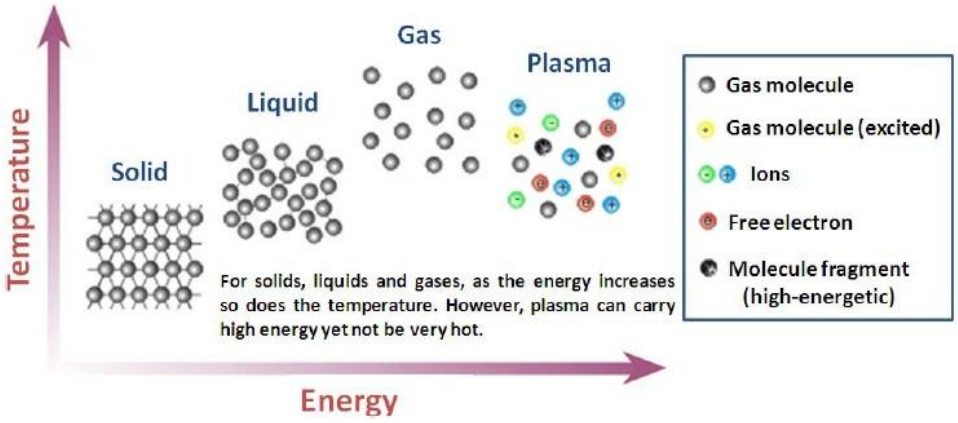

Figure 10. Relationship between temperature and energy [19].

Ensinass et al. studied the surface modification of composites using atmospheric pressure plasma treatment in order to improve the adhesive bonding. The results obtained showened that while using APPT treatment the exctraction of elements from the surface it is not significant. However with this technique it is possible to increase meaningly the oxygen content, increase the surface energy and also the wettability.[47]

2.4.1. Plasma classification

Plasmas are highly reactive species that are able to interact with any surface which they contact. By choosing the right configuration and processing parameters we can classify the plasma by its specific effects on the surface. Depending on the way, plasmas are activated and their working power, they can generate low or very high "temperatures" and are referred as non-thermal (i.e. cold) or thermal plasmas.

2.4.2. Atmospheric Pressure Plasma (APP)

The techniques for producing stable plasmas at atmospheric pressure have been known since the late 19th century. In the past decade, however, there has been a burst of research activity due to the unique effects and utility of the plasmas in the processing of industrial materials. Special attention is given on improving adhesive

bonding strength and paint adhesion on polymers, particularly as a tool for activation, cleaning (i.e. contaminants removal) and increasing surface energy (i.e. by changing the surface structure).

2.4.3. APP effects on the substrate

APP systems provide four major effects on surfaces, namely surface cleaning, surface activation, coatings and etching.

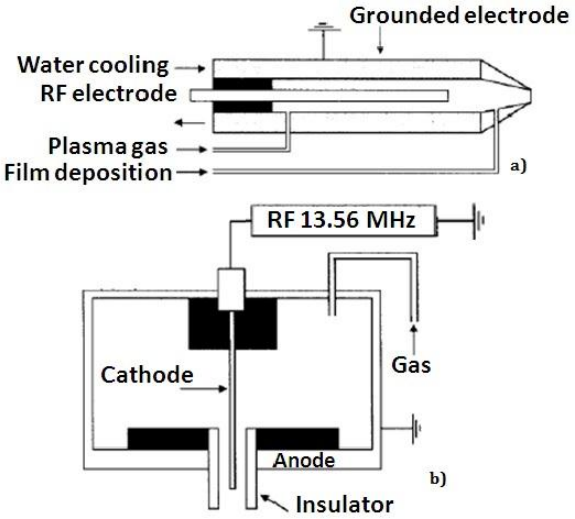

Figure 11. Cold plasma jets: Atmospheric pressure plasma jet (a) and Cold plasma torch [19]

2.4.3.1. Plasma Surface Activation

Surface activation consists on making energy available at the surface for adhesion promotion. This method uses the UV radiation and active oxygen species from the plasma break up separating agents, silicones and oils from the surface. Active oxygen species (radicals) from the plasma bind to active surface sites all over the material, creating a surface that is highly 'active' to bonding agents.

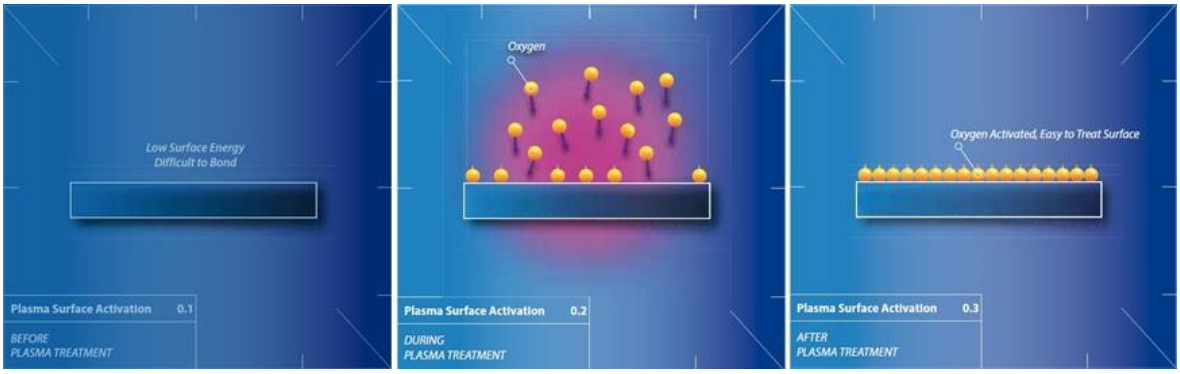

Figure 12. Plasma surface activation process [20].

Chapter 3: Materials and Methods

3. Materials and Methods

3.1. Materials

All chemicals used were commercially available and used without further purification. Titanium (IV) isopropoxide (97%), Acetylacetone (AcAc, > 99, 5%), Trimethoxyphenylsilane (97%), Isopropyl alcohol (> 99, 7%), Nitric Acid (ACS, 70%) and (3-Glycidoxypropyl) trimethoxysilane (>98%) were purchased from Sigma-Aldrich. The water used in all experiments was deionized water. SEEVENAX 315-02 (Resin) and SEEVENAX 315-00 (Hardner) were provided by Mankiewicz GmbH. The aluminium alloy, AA2024 – T3 (Al 90.7-94.7%; Cr max 0.1%;Cu 3.8 - 4.9 %; Fe max 0.5%; Mg 1.2-1.8%; Mn 0.3 - 0.9%; Si max 0.5%; Ti max 0.15; Zn max 0.25, Other metals 0.20%), used during this work was supplied by Airbus Innovation Group (Deutschland) and cut into appropriate dimensions for the different analyses of the anticorrosive properties. The CFRP HexPly®M21E samples used during this study was supplied by Hexcel (Deutschland).

3.1.1. Synthesis of the nanocontainers

The synthesis of the nanocontainers was performed by the University of Aveiro. It is a slow process where a mixture of 0.5 M of magnesium nitrate and 0.25 M aluminium nitrate deaerated solution (V=200 ml) is added to 1.5 M sodium nitrate deaerated solution (V= 400 ml) under continue stirring. A crucial parameter from this synthesis it is the pH from the solution. The regulation of the pH value is done throught a 2 M NaOH solution which allows to keep it between 7 and 9 during the all process. During 4 hours under 100°C degrees the LDH structure was formed and for this solution the pH value was preserved between 9 and 10. The nanoconatiners were delivered in a slurry state.[25]

In the case of the Bentonite it was used as a nanocontainer for Cerium III without any further treatment or purification.[25]

3.1.2. Inhibitors intercalation

This procedure, done in the University of Aveiro, was performed by anion-exchange method. Solutions with 0.1M concentration of the inhibitors were prepared. The pH value was adjusted for each type of inhibitor during the formation of the ionic form of the inhibitor. About 20 g of LDH slurry were added to 125 ml of the formed solution. The mixture was kept for 24 hours under continuous stirring. The formed slurry of LDH loaded with inhibitor was centrifuged at 10000 rpm during 90 sec and washed with deionized water three times

The bentonite nanocontainers were loaded with Ce^{3+}. On the first step a solution of Ce^{3+} (0.56 mol/L) in deionized water was prepared (40 ml) and stirred until all the salt is completely dissolved. The obtained solution was combined with bentonite (2 g) and continuously stirred during 24 hours. After this, the solution was filtered with vacuum filtration technique and washed with deionised water.[25]

3.2. Analytical methods and apparatus

Our goal, in this first part is to discover how much nanocontainers we can incorporate into the coating and test the efficiency from this coating.

Taking into account the previous work done in this field the techniques that will be used are: Electrochemical Impedance Spectroscopy (EIS), Salt Spray Test (SST) Adhesion Testing, Scratch Resistance and Drop Test.

In the following paragraphs the importance of each technique will be explained.

3.2.1. Electrochemical Impedance Spectroscopy

Electrochemical Impedance Spectroscopy (EIS) is a powerful non-destructive technique for the characterization of electrochemical systems. With a single experimental procedure encompassing a sufficiently broad range of frequencies, the influence of the physical and chemical phenomena may be isolated and distinct at a given applied potential. When applied to an electrochemical system, EIS can provide information on reaction parameters, corrosion rates, oxide characteristics and integrity, surface porosity, coating integrity, mass transport, and many other electrode/interface characteristics [21]. Processes occurring in the electrochemical

system can have different relaxation constants and will as such manifest themselves in different frequency regions. For example, the impedance data of an organic coated metal in a corrosive electrolyte typically reveals the electrolyte resistance at high frequency, the barrier (capacitive) properties of the coating in the mid-to-high frequency region, the coating resistance at lower frequencies, or corrosion / diffusion processes at the low frequencies. It is a quite complex system to understand, but can generally be modeled by an electrical equivalent circuit.

The impedance is measured by dividing the applied voltage by the measured current response. The impedance can be represented by a complex quantity. The resulting impedance of this system is given by equation 11. This impedance is limited to $Z = R_s + R_p$ at low frequencies ($\omega \rightarrow 0$).

$$Z(\omega) = R_s + \frac{R_p}{1 + \omega^2 R_p^2 C_{dl}^2} - j\frac{\omega^2 R_p^2 C_{dl}}{1 + \omega^2 R_p^2 C_{dl}^2} \qquad \text{Eq.(11)}$$

The probed frequencies are 10^{-2}Hz -10^{6}Hz. The time constant (relaxation time) equals R_pC_{dl} and can be read from the maximum in the imaginary part of the impedance. The phase of the impedance is given by equation 12.

The phase angle equals zero for pure resistive behavior,+90 degrees for pure capacitive behavior and -90 degrees for pure inductive behavior.

$$\theta = \arctan\frac{Z_{imaginary}}{Z_{real}} \qquad \text{Eq. (12)}$$

The value for the impedance at low frequencies correspond to $R_p + R_{cp} + R_s$ and can be used as a possible indicator for the coating performance.

3.2.2. Salt Spray Test

Salt Spray testing is conducted to determine the products resistance to corrosion; it is often conducted at the product level to provide quick feedback on coatings. Sometimes referred to as salt fog, or corrosive atmosphere testing salt spray testing encompasses a wide variety of test standards and methods, depending upon product application.

This test will be performed according to EN ISO 9227. Under these conditions:

3.2.3. Adhesion testing

Following the idea exposed in the paragraphe 2.4Plasma treatment adhesion is depending on the surface are improved wetting allows the adhesive of coating to penetrate the valleys and slopes od the surface typography providing a significant increase in bonding are.

This greatly increases the strength of the bond. To prepare the polymer surface fro improved paint or coating adhesion ASTM scratch test is used to determine the quality of the adhesive bond.

This technique will be performed in specific machine (ERICHSEN TESTING EQUIPMENT) and this equipment allows making precise scratches with 1mm of distance between each other.

The tape test is carried out for the metallized samples in the following way : The cloth tape tesaband® Premium 4651 is adhered to the metal layer, manually laid down and after about 60 seconds application time pulled off at an angle of 60 ° to the surface within 0.5 to 1.0 seconds, as Figure 13 shows. This test is used as the first indicator for a non sufficient adhesion of the coating. If a metal layer separation already can be determined, the adhesion must be rated as inadequate.

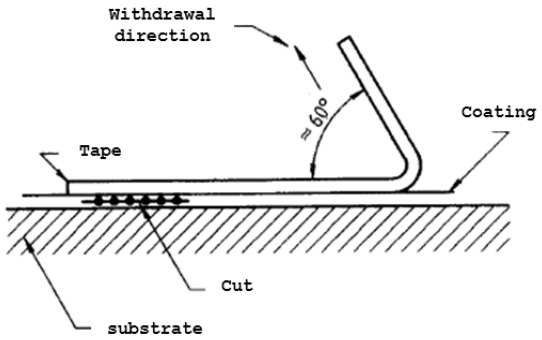

Figure 13. Withdrawal direction of the adhesive tape. [43,44]

With the cross-cut test, which was performed according to DIN EN ISO 2409:2013 (coating material - Cross-cut test), the adhesion of the metal layer can be evaluated more precisely. The norm specifies a test method to estimate the resistance of a coating against separation from the substrate. This is, however, no adhesive strength measurement. The procedure for the cross-cut test is as follows: With the Erichsen Testing Equipment 430P-I a continuous grid of six cuts in each direction is cut in the metal layer. The cutting distance for hard substrates with layer thicknesses up to 60

µm is 1 mm, for substrates with layer thicknesses between 61 µm and 120 µm 2 mm. It must be ensured that the cuts through to the substrate. Subsequently the cloth band tesaband® 4651 Premium gets glued to the grid again, manually laid down and after about 60 seconds application time pulled off in an angle of 60 ° to the surface within 0.5 to 1.0 seconds. The test result is then assessed with a cross-cut value according to the classification shown in Table 1 whereas in the range of this work only the cross-cut values GT 0 and GT 1 are classified as adequate adhesion.

Table 1. Classification of the cross-cut test - DIN EN ISO 2409:2013

Cross cut value	***Description***	***Surface cross cut section***
GT 0	The cutting edges are completely smooth; none of the Squares of the grid is detached.	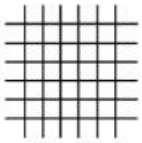
GT 1	The intersections of the grid lines show small chips of coating. Delaminated area doesn't exceed 5 % of the cross-cut area.	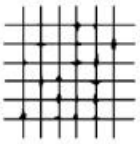
GT 2	The coating is detached along the cutting edges and / or at the intersections of the grid lines. Delaminated area greater than 5%, but not greater than 15% of the cross–cut area.	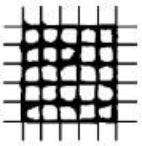
GT 3	The coating is partially or entirely chipped in wide strips along the cutting edges and / or some squares have partially or completely chipped. Delaminated area greater than 15%, but not greater than 35 % of the cross-cut area.	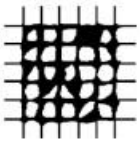
GT 4	The coating is chipped in wide stripes along the cutting edges and / or some squares are entirely or partially chipped. Delaminated area greater than 35%, but not greater than 65% of the cross-cut area.	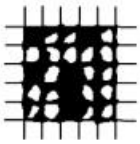
GT 5	Any delamination, that can not be classified as cross-cut value 4 anymore.	-

3.2.4. Scratch Resistance

This method determines under defined conditions the resistance of a single coating or multi-coat paint system, varnish or related product to penetration by scratching with a hemispherically tipped needle. The needle will penetrate the substrate, except in the case of a multi-coat system, where the penetration of the needle may be either to the substrate or to an intermediate coat. This technique will be performed regarding the EN ISO 1518.

Chapter 4: Experimental

4. Experimental

4.1. Assembly design

After a careful analysis of the work performed by other colleagues, it was verified the existence of certain problems in the assembly proposed by them. Since this is a crucial factor of the whole project, due to the need for systematic results, another approach to the assembly was elaborated. The main problem from the previous assembly was reproducibility of the tests.

During the assembly process some manufacturing problems arised. It was necessary to take into account the following aspects:

- Activation of the samples bottom edges in order to connect the copper wire.
- Isolation of all the edges applying a blue masking laquer.
- Avoid the gap/step between the two samples.
- Equalize the thickness from both samples.
- Avoid the electrolye pool in the bottom of the assembly.
- Two different approaches to connect the copper wire

This assembly should be:

- Reusable;
- Corrosion resistant;
- Easy to transport;
- Easy to do.

The sketch for this assembly was done through SolidWorks software as Figure 14 shows, this assembly it is composed by four pieces of PMMA:

- the first one, the big one, with 100 x 70mm will support the other pieces and the specimens;
- the second piece with 100 x 12 mm have two holes with 9.87mm of diameter, this part is very important because it will ensure that the specimens will be flat.

– The others two pieces 12 x 12 mm with 9.87 mm diameters will be spot for support for the top of the assembly.

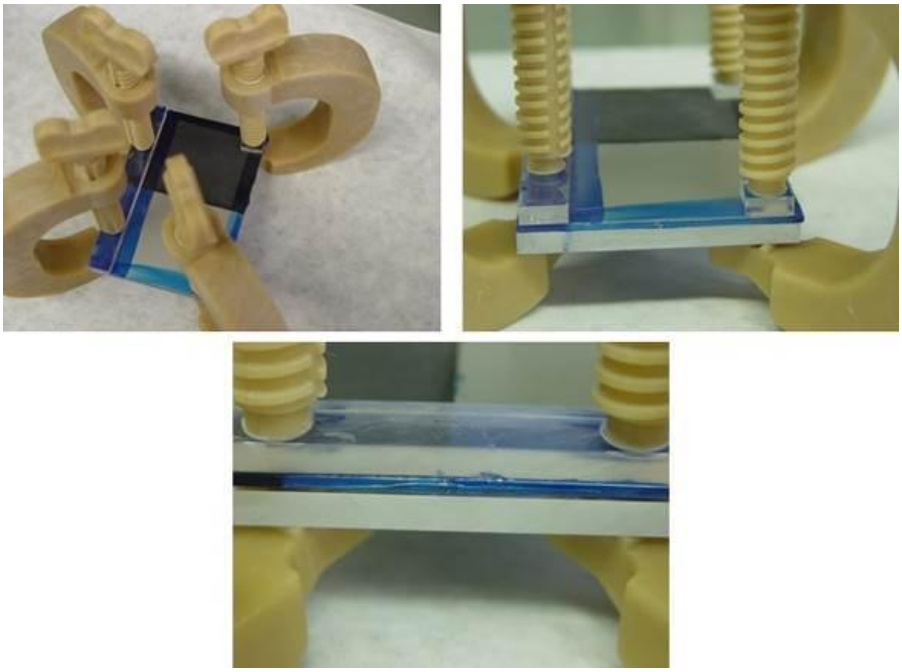

Figure 14. Assembly of the coupled samples.

To finish this assembly it is required clamps to hold all the pieces together, these clamps are made from inert material, as the Figure 14 shows. The Figure 15 and Figure 16 show in detail the structure from the assembly.

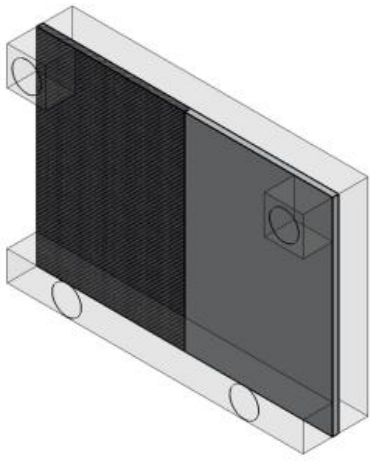

Figure 15. Assembly sketch supported by Solidworks.

After the results from the SST the samples coated with epoxy paint an improvement of the assembly was proposed as it can be seen on the Figure 16.

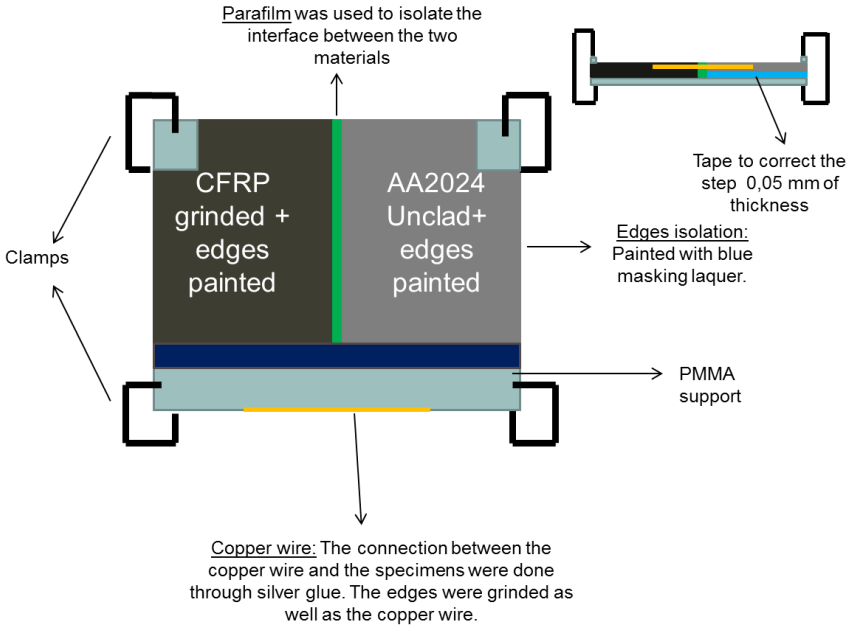

Figure 16. Detailed scheme from the assembly.

4.2. **Coating Systems**

This study is based in two major systems of coatings that can be divided in 4 sub-systems each as the schemes from Table 2 and Table 3. Sol-gel coating system shows. The coating systems were applied into two types of materials: aluminium alloy, AA2024 – T3, and CFRP, HexPly®M21E. Each material received a specific pre-treatment. The aluminium alloy got a Socosurf treatment and the CFRP got an Atmospheric Pressure Plasma.

4.2.1. Epoxy Paint

As the Table 2 shows the epoxy paint is a combination of a resin with a hardener, it is applied through spray coating. The coating and curing of this system was carried by an external company.

Table 2. Epoxy coating system.

Epoxy Paint	**Systems**	Reference (without nanocontainers)
		16% wt. LDH
		8% wt. LDH + 8% wt. Bentonite
		16% wt. Bentonite
	Parameters	**Paint:** SEEVENAX 315-02 (Resin) combined with SEEVENAX 315-00 (Hardener)
		Application: Spray
		Pre-treatment: Plasma treatment (only for CFRP) and Socosurf (only for AA2024)

4.2.2. Synthesis of sol-gel

The main purpose of the films applied through the pre-treatments on the alloy is to increase the adhesion between the metal and the organic paints. In addition the films must provide some degree of barrier protection. Therefore the approach of the sol-gel synthesis is based on the combination of different functionalized reagents used to build a system with tailored properties.

Yasakau et al. studied this sol-gel system and the results obtained were positive so for this work the same system will be used.[12] In the present work epoxy-functionalized silane (GPTMS) and metalorganic compounds (Ti alkoxides) were used as main

components of the sol-gel systems. GPTMS has epoxy groups that are compatible with the paint formulations used in industry. The epoxy groups can easily react with the functional groups of paints and provide necessary adhesion.

In addition the silicon alkoxy group can be hydrolysed and chemically bonded to the metal surface thus providing adhesion to the metal. Metalorganic compounds play a role of inorganic network formers. Oxide nanoparticles can be formed after partial hydrolysis of metalorganic precursors. These nanoparticles reinforce the coating matrix making it harder and denser. Table 3 shows all the parameters involved in the sol-gel synthesis.

Table 3. Sol-gel coating system

Sol-gel	**Systems**	Reference (without nanocontainers)
		16% wt. LDH
		8% wt. LDH + 8% wt. Bentonite
		16% wt. Bentonite
	Parameters	**Main precursors:** Titanium, GPTMS and PTMS
		Application: Dip coating
		Pre-treatment: Plasma treatment (only for CFRP) and Socosurf (only for AA2024)

Titanium based sol-gel system was synthesized according to controllable sol-gel route mixing two different sols. The first sol (sol 1) was obtained by controlled hydrolysis of titanium-isopropoxide, 97% (TPOT) solution in isopropyl alcohol (> 99, 7%) mixed with a complex agent at 1:4 molar ratio. The hydrolysis was performed under stirring by a magnetic stirrer and in a water bath at a constant temperature of 22 ° C

After 20 min which were necessary to obtain complexation of the metalorganic precursor, 0.5ml of water with pH 0.5 (HNO_3 was used for acidification; pH ~ 0.5) was added for hydrolysis and condensation, which continued for 60 min.

Acetylacetone was used as complex agent in this synthesis to reduce the reactivity of metallic alkoxides.

The second sol (sol 2) was prepared by hydrolysis of 3-glycidoxypropyl trimethoxisilane, 97% (GPTMS) combined with phenyltrimethoxysilane (PTMS)

solution in the presence of a small amount of acidified water. The hydrolysis was performed under stirring by a magnetic stirrer for 60 min and in a water bath at a constant temperature of 22 ° C

The third hybrid solution was obtained by mixing the titanium-based sol with the organosilane-based one at a 1:2 volume ratio.

The final sol-gel solution was performed under stirring by a magnetic stirrer for 1 h, in a water bath at a constant temperature of 22 ° C, and then aged for 1 h. [12]

The nanocontainers were incorporated into the coating after the solution 3 is obtained, as Figure 18 shows.

Figure 17. Illustration of the sol-gel synthesis.

Figure 18. Addition of nanocontainers in sol-gel.

Table 4. Sol-gel formulations

Sample Name	TPOT (sol1) ml	AcAc (sol.1) ml	Water (sol.1) ml	GPTMS (sol.2) ml	PTMS (sol.2) ml	Water (sol.2) ml
Sol-gel coating	29,825	22,331	7,805	59,858	50,224	29,268

4.2.2.1. Dip coating

The sol-gel films were applied by dip-coating using a BAHR Modultechnik type ELZ 60 2003, chemically cleaned aluminium substrates with immersion time in the sol-gel of 41 seconds followed by controlled withdrawal with a speed of 18cm/min. Cross-linking, gelation and solvent evaporation of the produced sol-gel was carried out in an oven afterward. The humidity was controlled throughout the whole process and it was always around 25%.

4.2.2.2. Curing

The coated samples were dried 30 min at room temperature and then put in the oven. The curing cycle is explained in Figure 19 When ready, the oven slowly cools down to room temperature.

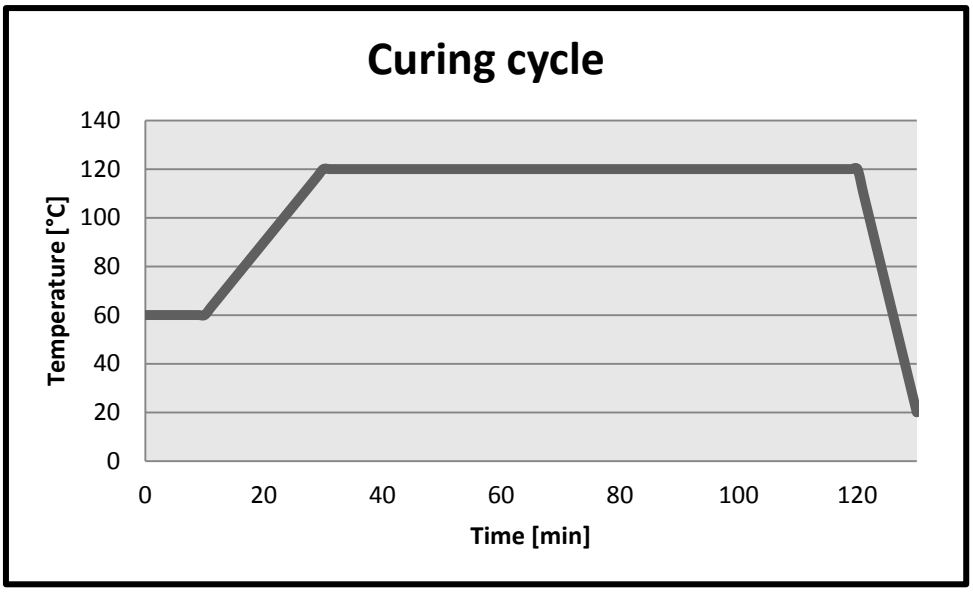

Figure 19. Curing cycle for the sol-gel samples.

4.2.3. Paint preparation

In order to test the compatibility of the epoxy paint with the substrate some of the samples were coated with a bar coater. This is not the most precise method because the thickness of the coating is not homogeneous, but for a first trial it can be acceptable.

Table 5. Epoxy Paint formulation.

	Reference	8% LDH loaded with BTA combined with 8% Bentonite loaded with Cerium	16% Bentonite loaded with Cerium
Resin (g)	103,7	22	21
Bentonite (g)	-	2,1	3,4
Stirring time (min)		5	5
LDH (g)	-	1,8	-
H2O	-	5,4	4,6
Hardener (g)	41,3	9	9
Speed (rot/min)	120	120	200
Stirring time (min)	-	5	10
Resting time (min)	-	25	20

Before proceeding to the coating, a dispersion test was done. The dispersion was good for every system without agglomerations and good homogeneity as Figure 20 shows. In some cases we had some bubbles due to the mechanical stirring, but they disappeared after a while.

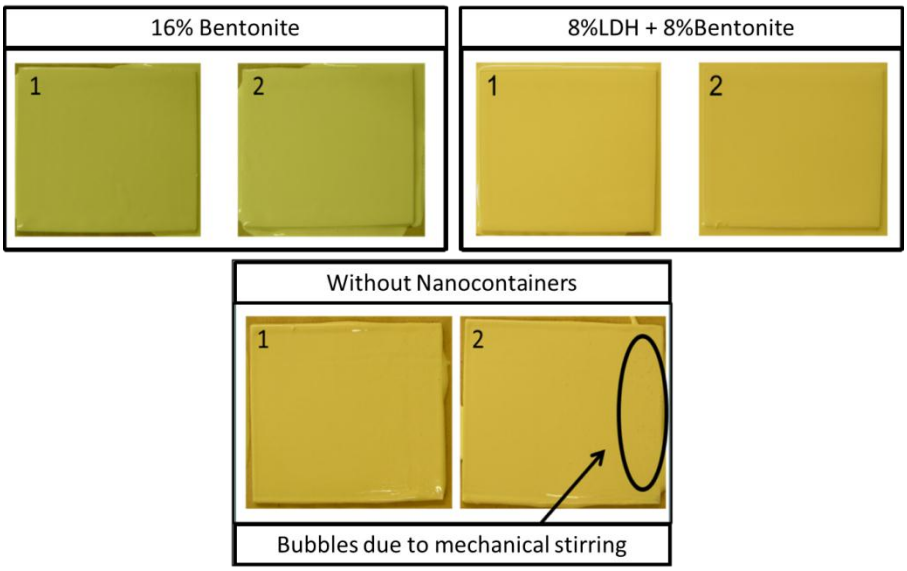

Figure 20. AA2024 samples coated with epoxy paint using a bar coater.

4.3. **Prove the principal of galvanic effect**

In order to test the efficiency of the assembly a SST was performed:

- Sample 1: CFRP specimens (70x50mm) as received + AA2024 specimens (70x50mm) with TSA anodic film and sealing,
- Sample 2: CFRP grinded + AA2024 with TSA anodic film and sealing
- Sample 3: AA2024 with TSA anodic film and sealing.

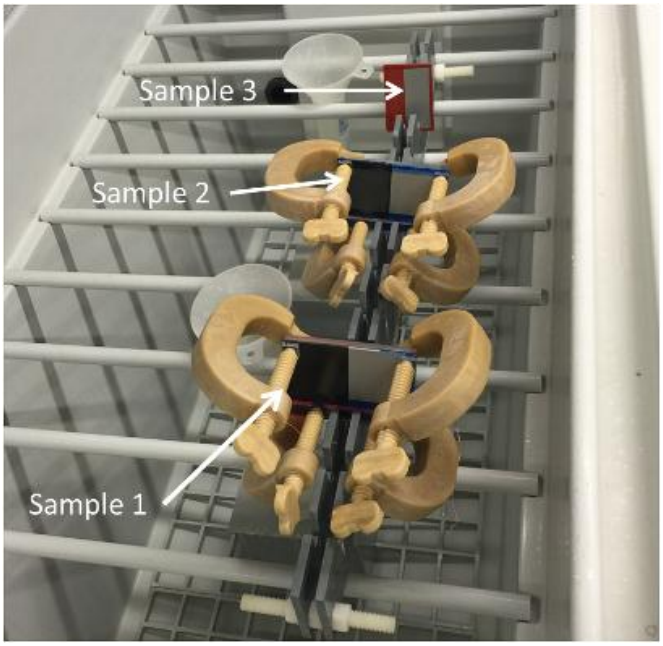

Figure 21. Samples used to prove the galvanic effect.

4.4. **Prescreening tests**

This procedure will tell us the behaviour of the paint when combined with the nanocontainers. It is necessary to evaluate the dispersion from the nanocontainers into the paint. The dispersion can be improved by changing some parameters, such as, stirring type, rotation, time and speed, as the Table 5 shows.

As Table 5 shows, it is possible to observe that the bentonites are more difficult to disperse so it was necessary to increase the stirring speed and time. In comparison with LDH the bentonite needs more solvent (water) in order to be well dispersed.

4.4.1. Drop test

A drop of a NaCl solution was applied inside the hole as Figure 24 shows. This measurement was executed inside of a isolation cabine in order to have a controlled atmosphere. Table 6 shows the parameters used in this process.

With this technique it is possible to have a first impression about the coating compatibility and the inhibitors efficiency, through the amount of corrosion products deposited during the time.

Table 6. Drop test parameters

Parameters	
Solution	3wt% NaCl
Tape Thickness	41 mm
Diameter tape hole	4mm
Diameter hole	2mm

In order to obtain a reasonable drop of electrolyte tape was added like the Figure 22 shows. The corrosion effect will be measured during a period of time 24h, 48h, 72h and 96h, as it can be seen in Figure 23 and Figure 24.

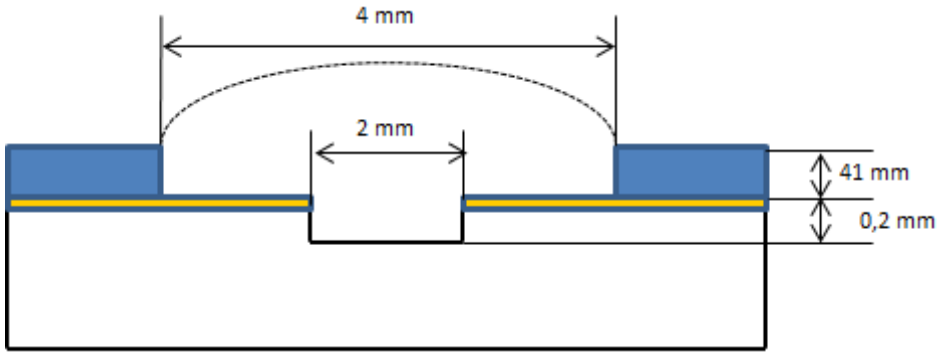

Figure 22. Scheme of a sample for drop test

This procedure was applied in both coating systems: epoxy paint and sol-gel. The samples were coated through a bar coater and the wet thickness of the coating was 25µm.

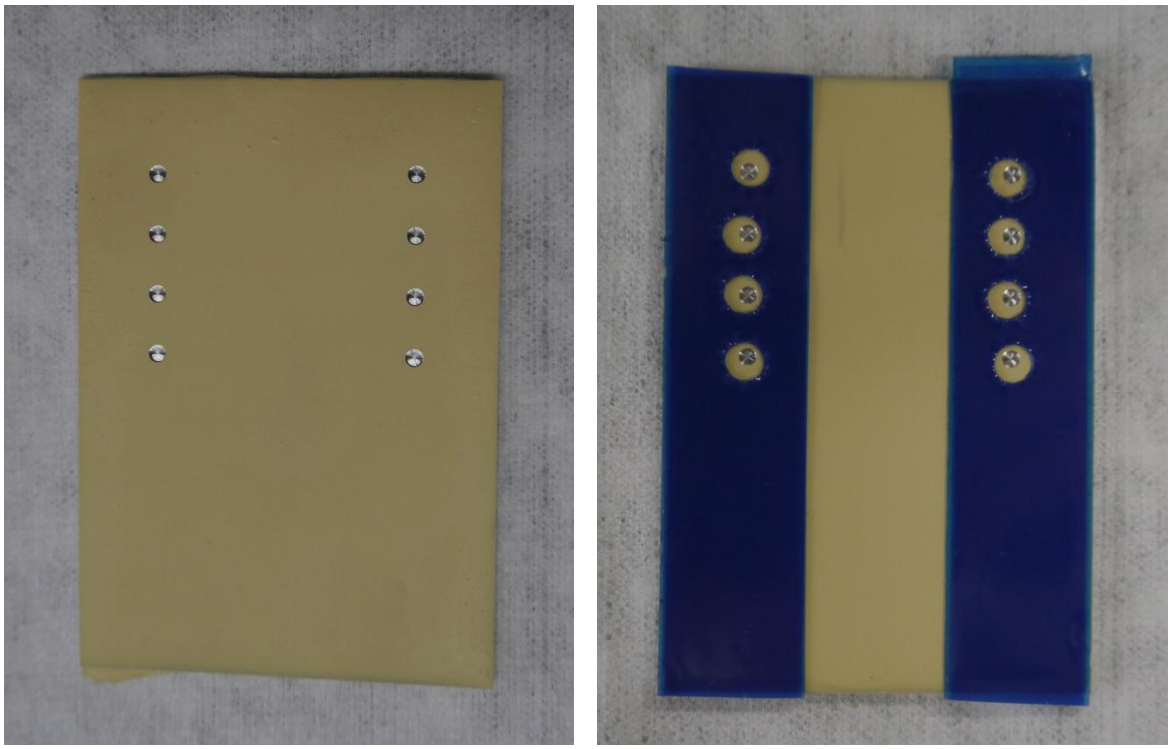

Figure 23. Drop test: stage 1 and 2.

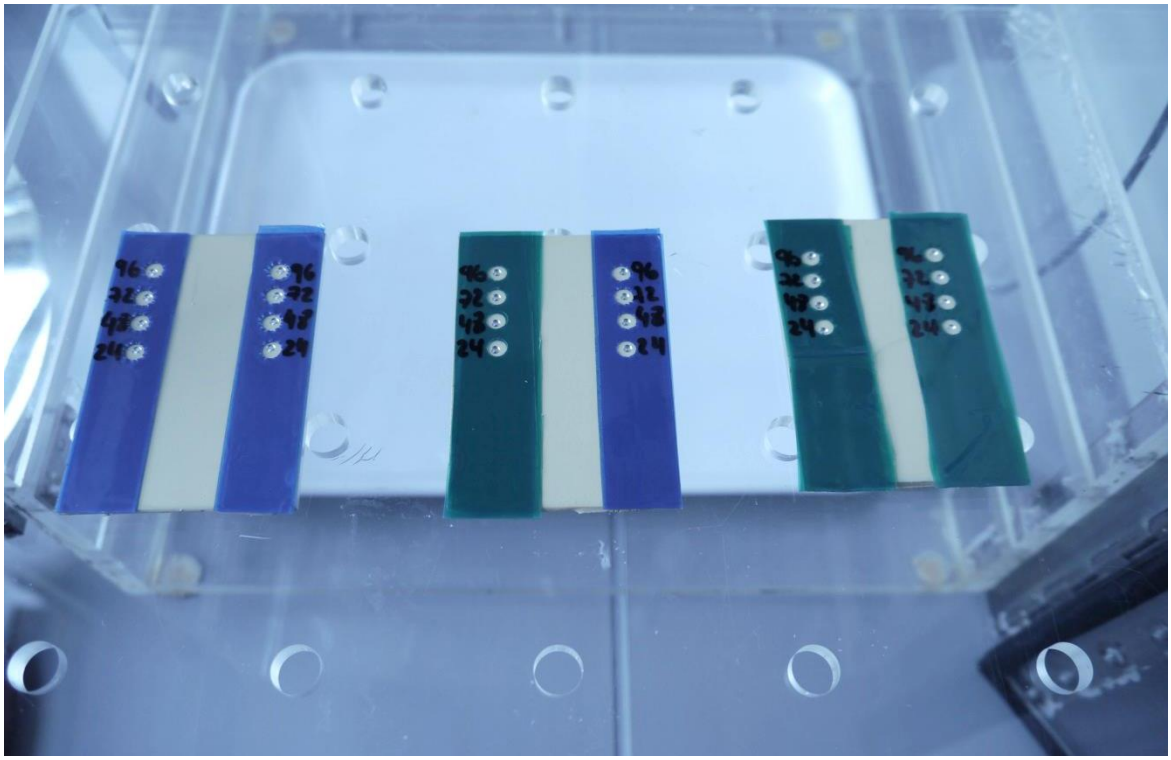

Figure 24. Drop test stage 3.

4.5. **Plasma treatment**

In order to improve the adhesion of the CFRP samples a plasma pre-treatment was done. Table 7 shows the parameters used during this procedure where R0 is the width, R1 is the length, R2 is the distance between pathways, R3 is the number of cycles, R4 is the Plasma-Substrate distance and R5 the substrate thickness. Also the atmosphere used during for this configuration was air, the frequency was 23 kHz, the power was 1000 W and the velocity was 120 mm/s.

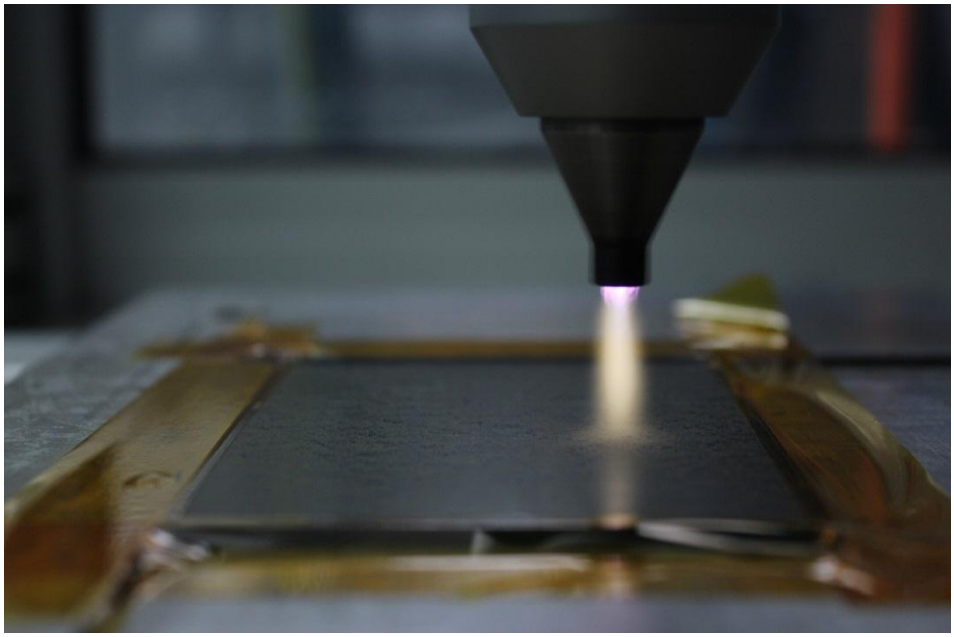

Figure 25. Plasma treatment of CFRP specimen.

Table 7. APPT parameters.

R0 [mm]	**R1 [mm]**	**R2 [mm]**	**R3 [ ]**	**R4 [mm]**	**R5 [mm]**
200	215	3	5	30	2

4.6. Corrosion tests

4.6.1. Salt Spray Test

For this specific test the samples have to be tilted approximately 10 degrees as Figure 26 shows. This test will be performed according to EN ISO 9227 under these conditions:

Table 8. Parameters of the Salt Spray Test.

Parameters	
Chamber temperature	35 ± 2°C
Salt fog fall out	1.5 ± 0.5 ml/h on 80 cm^2
pH of salt fog	6.5 – 7.2
Solution	50 g/l ± 5 g/l NaCl in de-ionized water

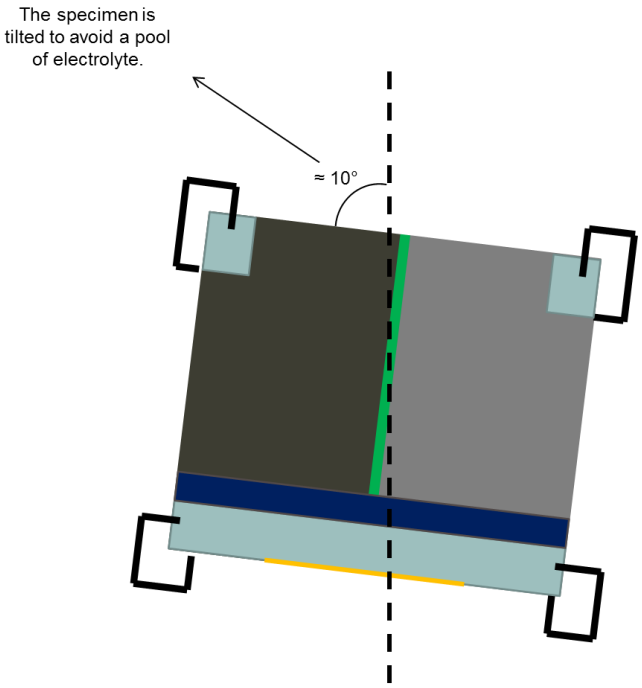

Figure 26. How samples were placed within the chamber.

4.7. EIS measurements

This technique was used to estimate the evolution of the corrosion protection performance of bare and coated materials during immersion in a NaCl solution with a concentration of 0.5M. The measurements were carried out at room temperature in a

farady cage. A frequency range between 10^{-2} Hz to 10^{5} Hz with 10 points per decade and 10mV AC perturbation amplitude vs. OCP were used. OCP acquisition was 180 seconds. The measurements were performed using a Gamry reference 600TM.

Chapter 5: Results and Discussion

5. Results

This chapter presents a study of the galvanic effect between AA2024 coupled with CFRP, the adhesion properties of the two types of coatings, corrosion test (SST), method of corrosion investigation (EIS). Two formulations of coatings were proposed and one is showing promising results. The study provided information about which formulation should be used in the future.

5.1. Prove of principal of galvanic test

The only sample presenting corrosion products is the sample 2 as Table 9 shows. This means that there is a galvanic effect so this kind of assembly can be used for further tests or tests for coupled painted specimens. The pits from the interface present a more advance level of corrosion and in addition there is a higher cooper deposition in this area as Figure 27 and Figure 28 show.

Table 9. Results from the SST test in order to prove the existence of galvanic effect.

Test Duration	**Sample 1 CFRP coupled as received**	**Sample 2 CFRP coupled grinded**	**Sample 3 AA2024 uncoupled with TSA**
24h	No defects	3 white spots on the surface related to pits	No defects
48h	No defects	3 pits on the surface, 3 pits on the interface	No defects
72h	No defects	3 pits (on the surface) with corrosion products and 7 pits on the interface	No defects
96h	No defects	3 pits with corrosion products and 7 pits on the interface	No defects
192h	No defects	3 pits, 14 pits on the interface	No defects

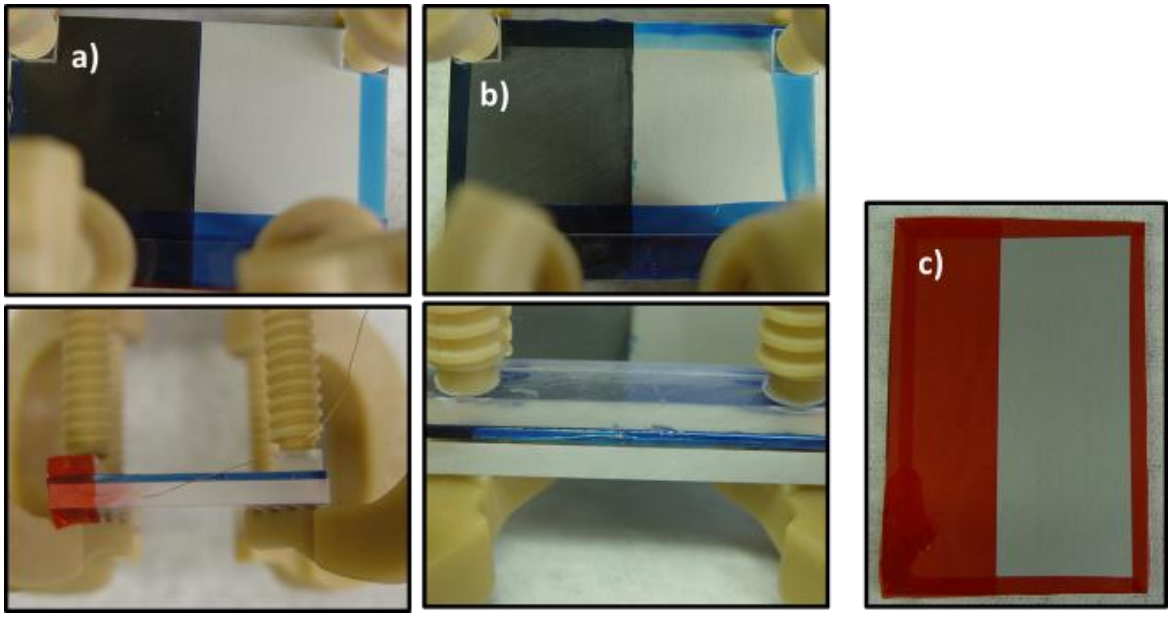

Figure 27. Samples used during the measurement: a) CFRP, as received, coupled with AA2024 with TSA treatment; b) CFRP, ground, coupled with AA2024 with TSA treatment and c) AA2024 uncoupled with TSA treatment.

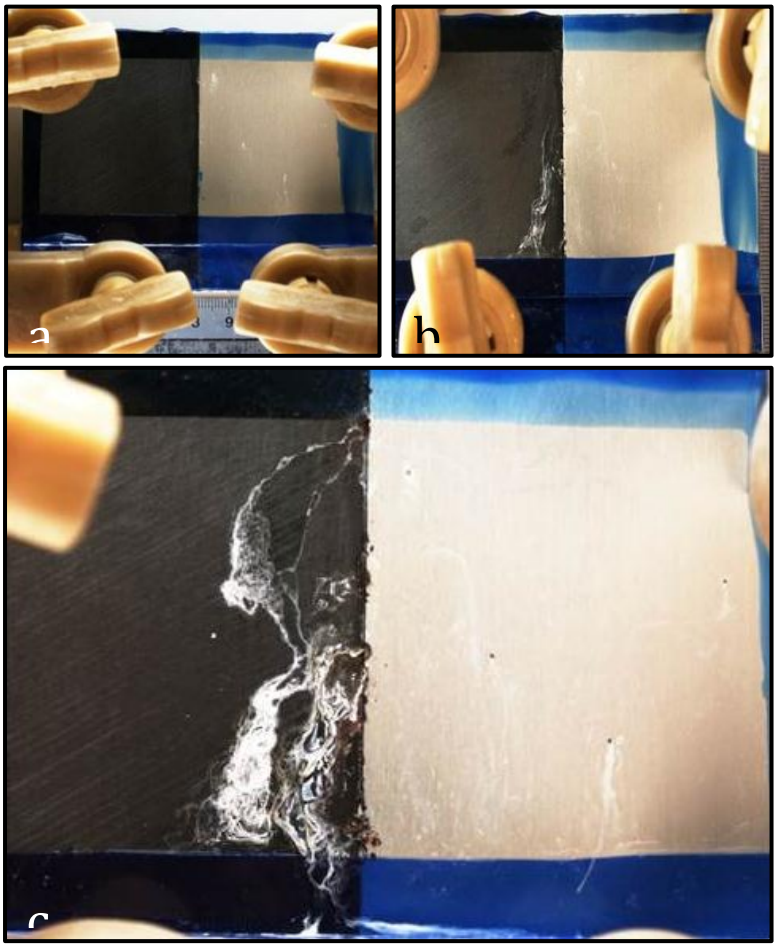

Figure 28. Photos of sample 2 (TSA pre-treatment) coupled with CFRP grinded samples (a) after 24h, (b) after 72h and after 192h in neutral salt spray test according to EN ISO 9227

5.2. **Prescreening tests**

Two batches of epoxy paint were prepared. The first one was used to perform the prescreening tests.

- **Adhesion and scratch test:**

The samples were indentified according to the pre-treatment and type of coating applied to them, thereby SCO stands for Socosurf treatment, EP for epoxy paint and SG for sol-gel coating. The evaluation was based on the information showed on Table 1. The results obtained before and after immersion demonstrate that the degree of adhesion is good and constant for both coatings, as it can be seen in Table 10.

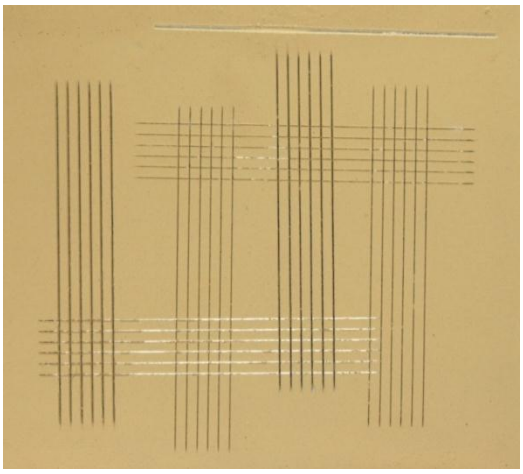

Figure 29. Adhesion test: AA 2024-T3 substrates coated with epoxy paint incorporated with 16% wt LDH loaded with BTA

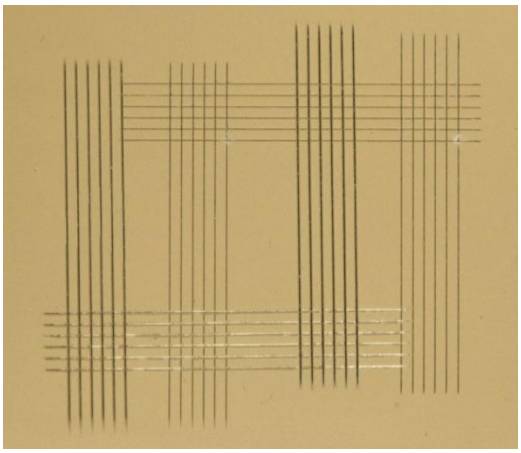

Figure 30. Adhesion test: AA 2024-T3 substrates coated with epoxy paint incorporated with 8% wt LDH loaded with BTA + 8%wt

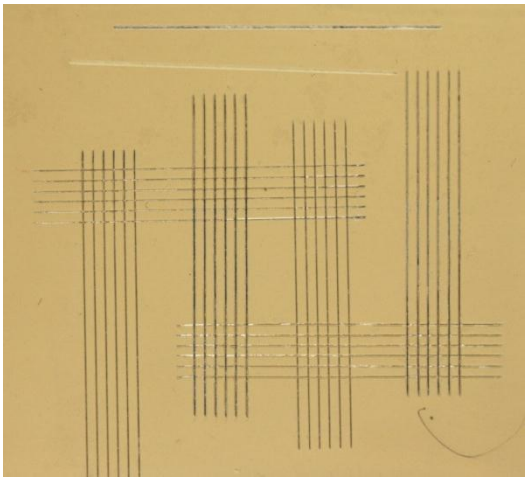

Figure 31. Adhesion test: AA 2024-T3 substrates coated with epoxy paint without inhibitors

Table 10. Adhesion and scratch results.

Sample	c(CeNO3) wt.%	c(BTA) wt.%	Before		After		Blisters	Scratch 1500 kg
			GT A1	GT B1	GT A2	GT B2		
SCOREF1	0	0	0	0	1	1	N	Y
SCOEP1	0	16	Not measured					
SCOEP2	0	16						
SCOEP3	8	8	0	0	1	1	N	Y
SCOEP5	16	0	0	0	1	1	N	Y
SCOSG1	0	0	0	0	0	0	N	Y
SCOSG3	0	16	0	0	0	0	N	Y
SCOSG5	8	8	0	0	0	0	N	Y
SCOSG7	16	0	0	0	0	0	N	Y

- **Drop Test:**

The evaluation of this test was based in:

- The amount of corrosion products
- Discoloration
- Gas bubbles.

Table 11. Results form the drop test in defects of epoxy coatings.

	Without inhibitors		8%LDH+8%Bent		16%Bent	
24h						
48h						
72h						
96h						

Taking the criteria mentioned above into account, the best result belongs to the samples coated with 8% of LDH loaded with BTA and 8% of Bentonite loaded with Cerium. This system is the one that presents the lowest amount of corrosion products.

5.3. **SST results**

During the Salt Spray Test the specimens were assembled in a special way, as Figure 14 and Figure 15 show. Figure 32 to Figure 34 show the evolution of corrosion in the different formulation from the epoxy paint. Over the time it was possible to observe that the presence of inhibitors makes the difference. In the sense that in the system

without any inhibitors the presence of corrosion pits is detected. The system with 16% wt LDH shows some pits and products of corrosion.

The morphology of the scratch causes a pool of electrolyte, generating additional corrosion products in the systems without inhibitors and 16% wt LDH loaded with BTA. This issue was amended for the next samples in order to avoid the high level of electrolyte.

The system incorporated with the combination of the two types of nanocontainers, LDH loaded with BTA and Bentonite loaded with Cerium, 8% each present different results after 72 hours inside of the salt spray chamber. This specimen presents intensive corrosion close to the interface with CFRP. This could indicate that the potential is higher close to the interface.

For the sol-gel coating the presence of corrosion products in the scratch is more intense than in the epoxy paint due to the corrosion pits in the surface. In all the systems the corrosion is more intense next to the interface with CFRP (left side of the picture) as expected.

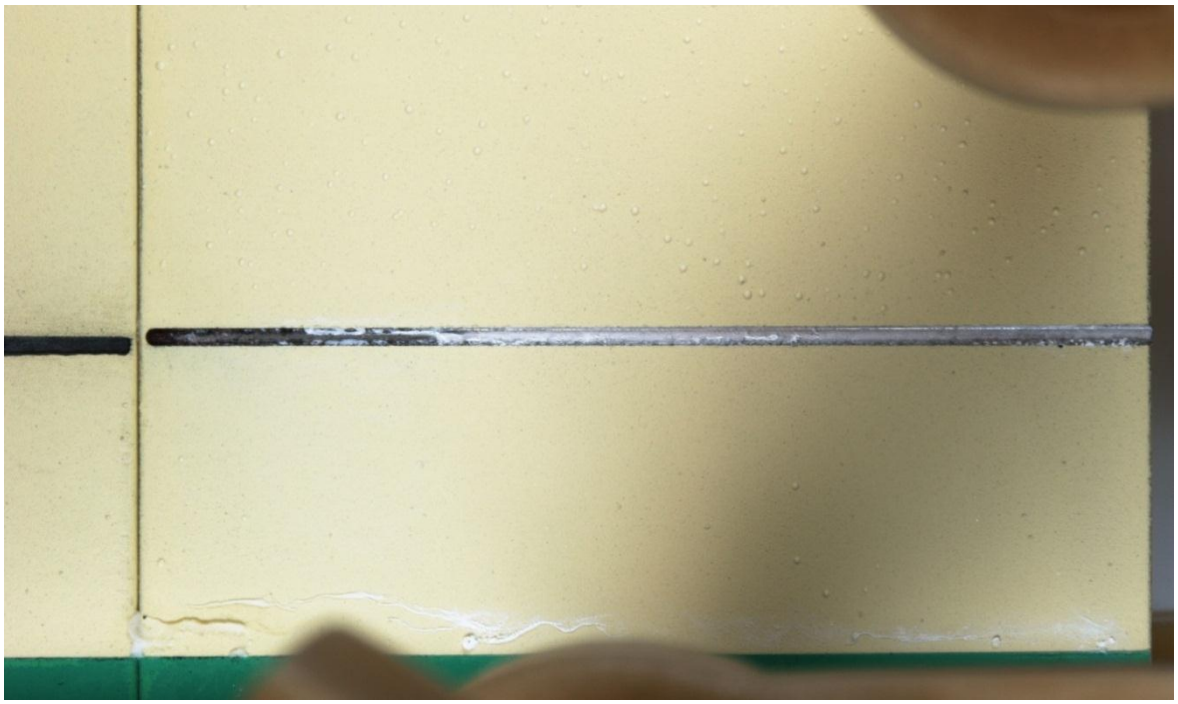

Figure 32. Results from the SST after 72h (samples coated with epoxy paint): 8% wt LDH loaded with BTA + 8%wt incorporated into the coating .

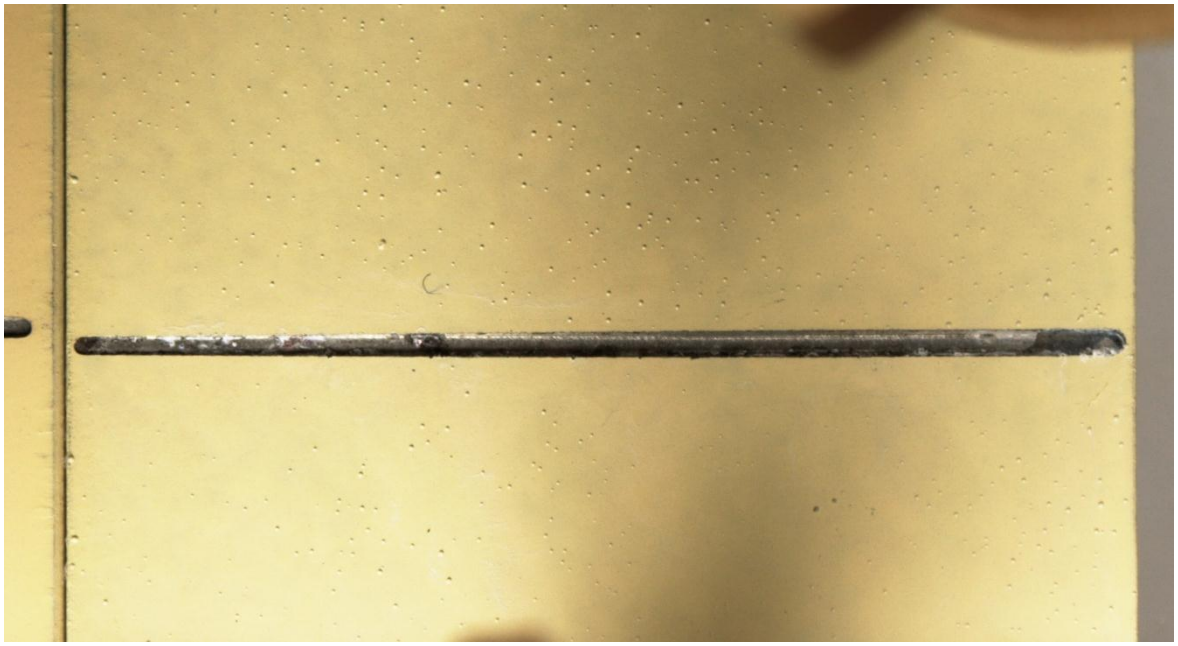

Figure 33. Results from the SST after 72h (samples coated with epoxy paint): 16% wt LDH loaded with BTA incorporated into the coating .

Figure 34. Results from the SST after 72h (samples coated with epoxy paint): without nanocontainers.

Figure 35 presents the three formulations prepared with the epoxy paint after every cycle of SST an optical analysis was perfromed.

As it can be seen in Figure 35a), the paint without any additives after 72 hours in the SST chamber does not show corrosion pits or products at the surface. However, the corrosion existent in the scratch is quite intense.

On the other hand, as shown in Figure 35b) and Figure 35c), the AA2024 specimen with inhibitors reveals blisters at the surface during the SST.

In order to understand the reason for the presence of these blisters, microscopic pictures were taken for coupled and uncoupled samples from the system with the combination of the two inhibitors. Thereby, it would be possible to understand if the appearance of this defect was caused by the coupling. As it can be seen in Figure 36 the blisters also appeared in the uncoupled samples.

The behaviour of the sol-gel coating under the same conditions was different. The coated surface from the system without inhibitors, Figure 37, shows no corrosion activity. On the other hand, as it can be seen in Figure 40 and Figure 39, where 16% wt of Bentonite and 8% wt LDH combined with 8% wt Bentonite were respectively incorporated into the sol-gel coating, there is no presence of blisters. Instead the sample is covered with corrosion pits.

The distribution of the pits is senseless in both cases, considering the galvanic effect. Taking into account the galvanic effect, the load of pits should be stronger where the surface potential value is higher. In Figure 40 the pits are more intense in the region away from the interface AA2024/CFRP. Also in Figure 39 the pits are more or less homogeneously distributed.

In the case, where the combination of the inhibitors was fulfilled, more corrosion pits occurred, not withstanding the intensitivity is higher for the case with 16% wt Bentonite.

Lastly the system represented in Figure 38 (16% wt. LDH) shows the best performance of all the systems tested. This fact can be explained with the existence of better compatibility between nanocontainers and coating.

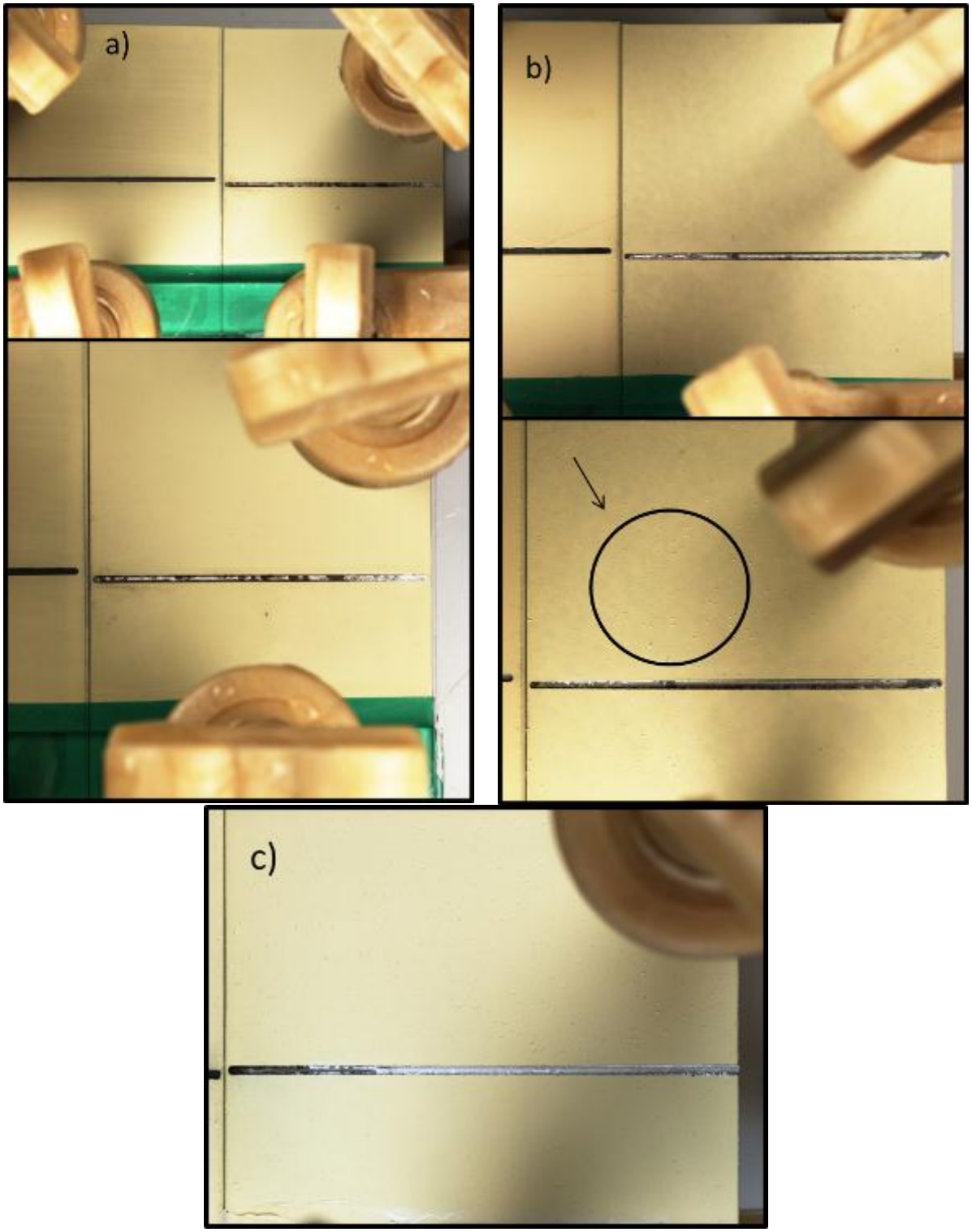

Figure 35. Assembly used during the SST (samples coated with Epoxy paint): a) without inhibitors; b) 16% wt LDH loaded with BTA and c) 8% wt LDH combined with 8% wt Bentonite loaded with Cerium incorporated into the coating after 72 hours.

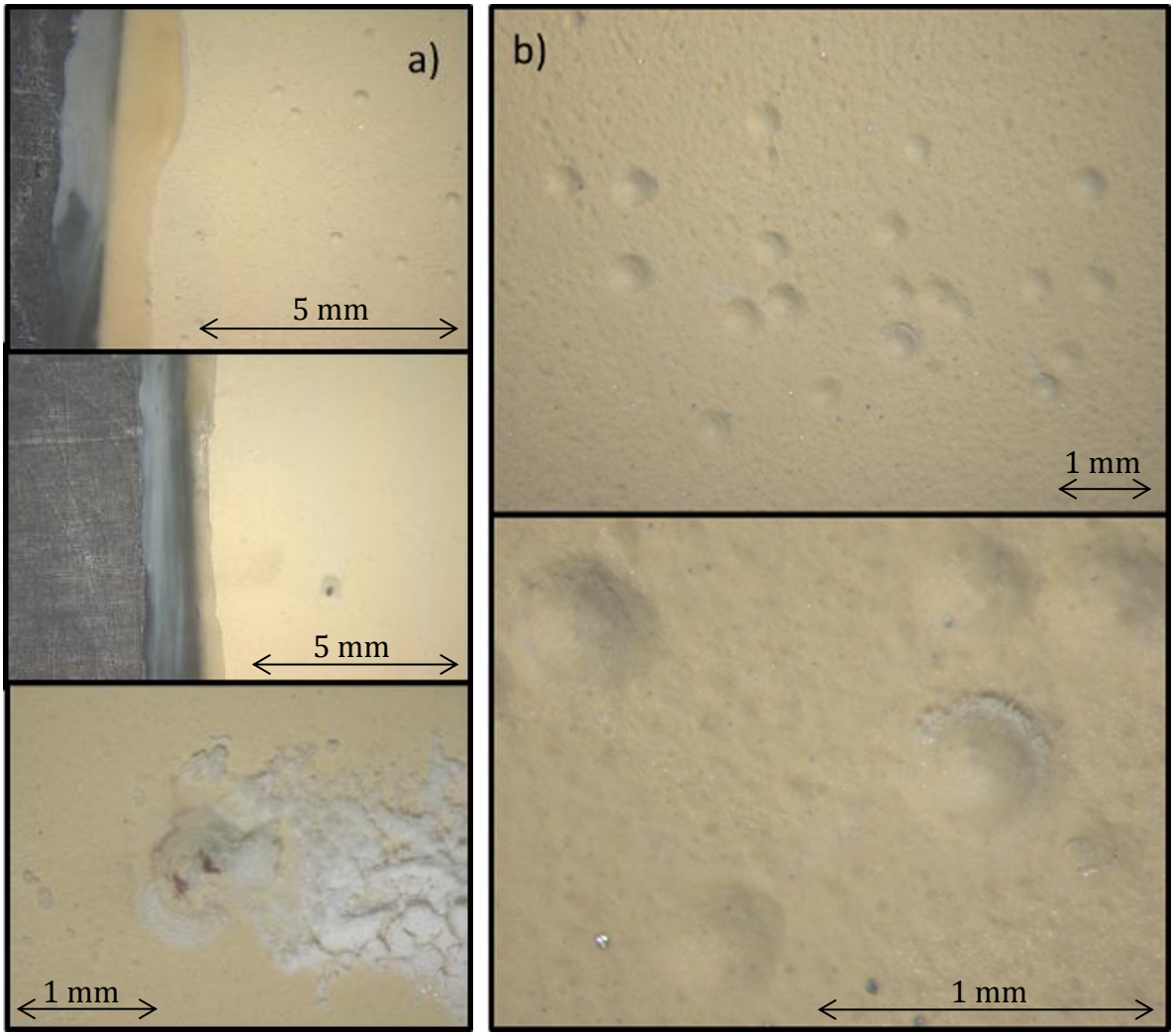

Figure 36. Microscopic pictures from the system 8%LDH loaded with BTA combined with 8%wt.Bentonite loaded with Cerium (Epoxy paint) after 144 hours in the SST chamber: a) AA2024 coupled with CFRP,b)AA2024 uncoupled.

Besides a low amount of oxygen and water transportation to the metal/coating interface the protective properties of barrier coatings result mainly from a prevention of ionic current flow through the coating. Exposure of organic coatings to electrolytes often leads to a development of blisters and decreasing substrate protection because of subcoating corrosion.

The blister formation between the coating and the substrate AA2024 – T3 is complicated due to the complex microstructure of the coating. The slowing of the oxygen reduction reaction is particularly essential. [45]

Because of its support of electron transfer reactions the cathodic intermetallic compound (IMC) is a bonding, on which the majority of cathodic reactions on

AA2024-T3 take place. If the space between the IMC was larger than the width of the delamination zone, the cathodic reactions on the cathodic IMC would still be uncapable of causing cathodic delamination. Other proposed mechanisms describing the growth of blisters are osmotic pressure, anodic undermining and corrosion product wedging.

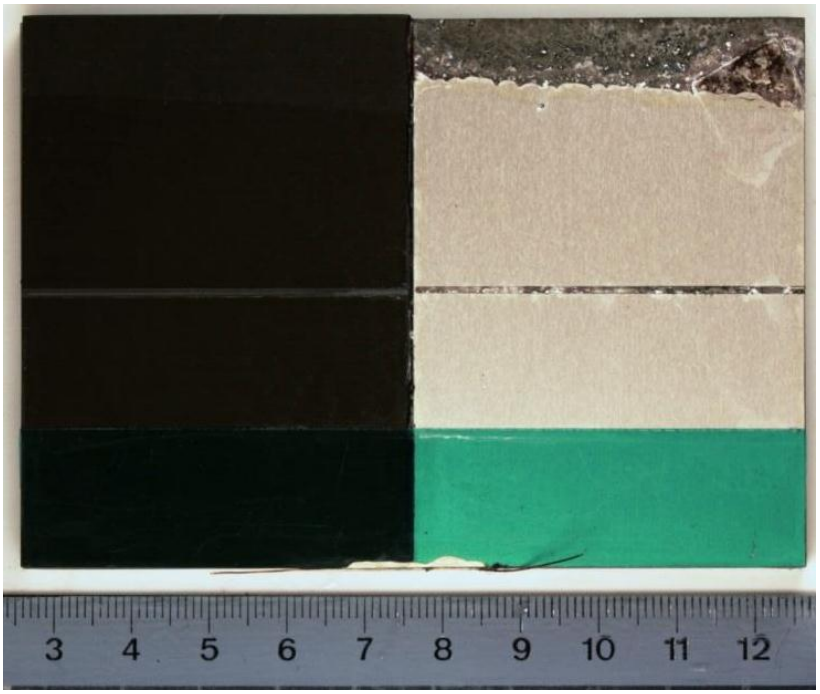

Figure 37. Assembly used during the SST (samples coated with sol-gel): without nanocontainers.

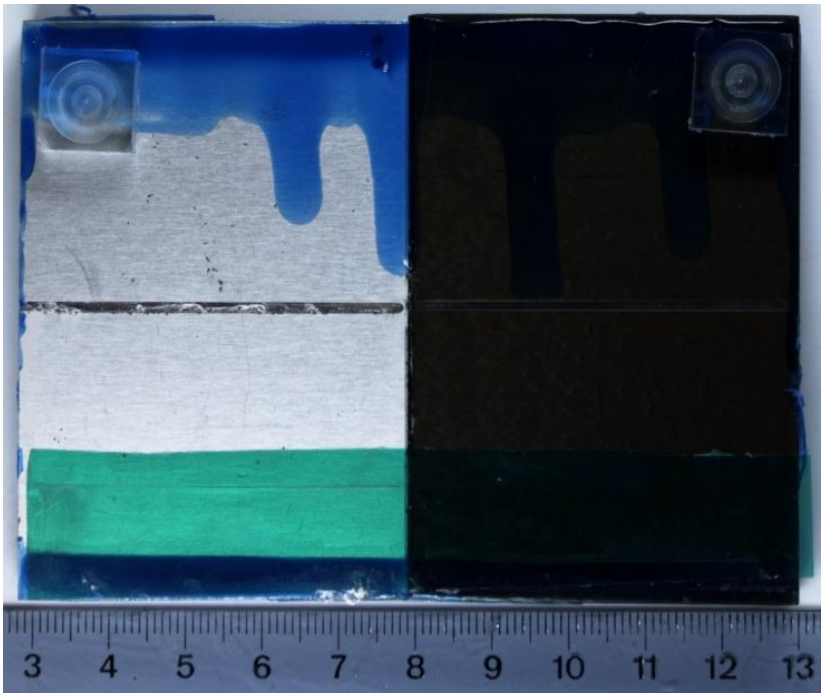

Figure 38. Assembly used during the SST (samples coated with sol-gel): 16% wt LDH loaded with BTA incorporated into the coating after 144 hours.

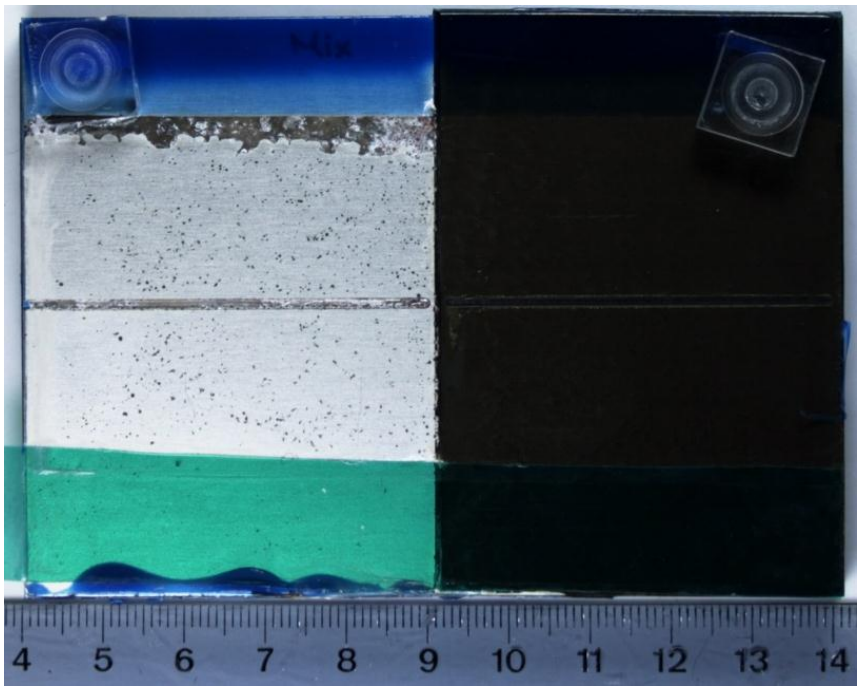

Figure 39. Assembly used during the SST (samples coated with sol-gel): 8% wt LDH loade with BTA combined with 8% wt Bentonite loaded with Cerium incorporated into the coating after 144 hours.

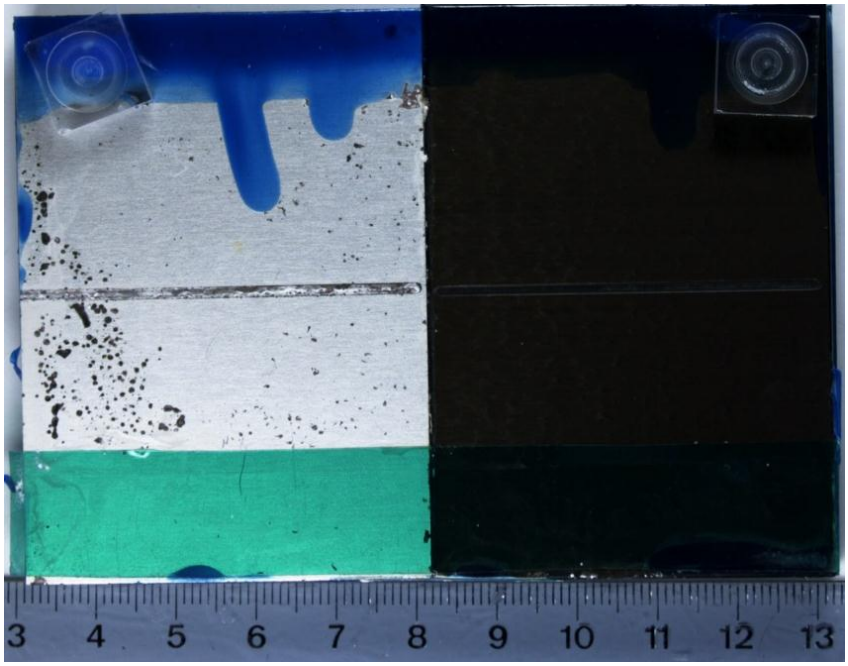

Figure 40. Assembly used during the SST (samples coated with sol-gel): 16% wt Bentonite loaded with Cerium incorporated into the coating after 144 hours.

5.4. **Impedance Results**

EIS technique was used to estimate the evolution of the corrosion protection performance of bare and coated AA2024 specimens during immersion in a NaCl solution with a concentration of 0.5 M.

The measurement was carried out at room temperature in a farady cage. A frequency range between 10^{-2} Hz to 10^{5} Hz with 10 points per decade and 10mV AC perturbation amplitude vs. OCP were used. OCP acquisition was 180 seconds. The measurements were performed using a Gamry reference 600TM. The measurements were performed on aluminium specimens (AA2024-T3) without defects.

The systematic EIS was done for all the coating systems listed in Table 2 and Table 3, for the following times of immersion: 0 hours (~ 20 minutes), 24 hours, 48 hours and 72 hours.

This section intends to show the effect of corrosion inhibitors when incorporated in coatings, while selected substrates are immersed into the base corrosive media – reference solution (0.5 M). The selected coatings were epoxy paint and sol-gel.

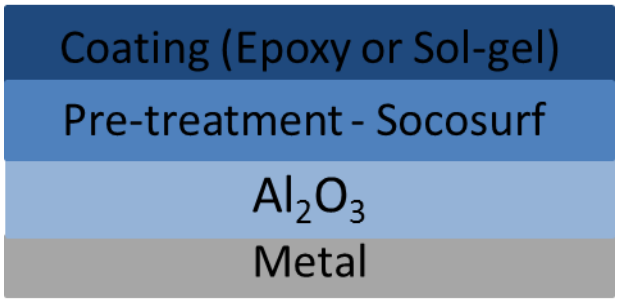

Figure 41. Scheme of the layers over the substrate.

5.4.1. Epoxy Paint

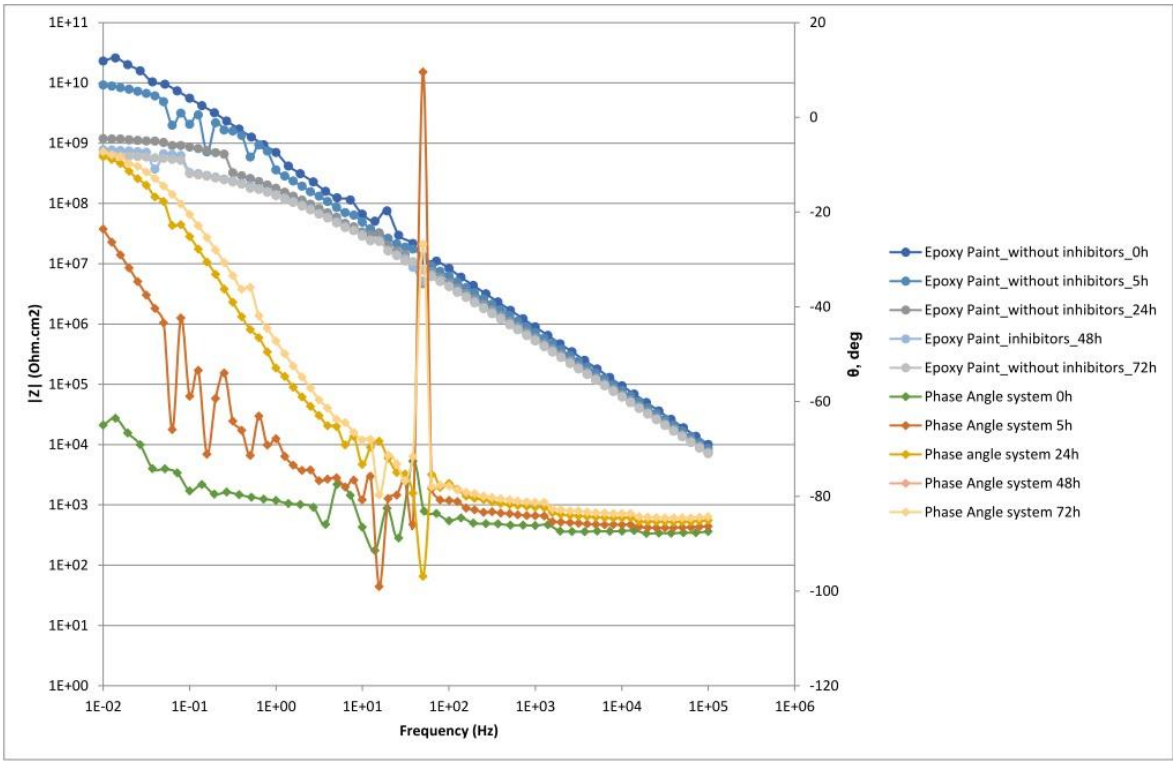

Figure 42. Impedance measurements of the specimens coated with epoxy paint without inhibitors.

In Figure 42, Figure 44 and Figure 45 the prepared formulations for the epoxy coating system are represented. These figures describe the evolution over time for each system. The equivalent circuit, which corresponds to the type of system used can be presented as follows (Figure 43).

Considering the epoxy paint results represented by Figure 42, the low frequency impedance of the coating decreases (from 10^{10} to 10^{9} ohm.cm^2) which is confirmed by the Table 12.

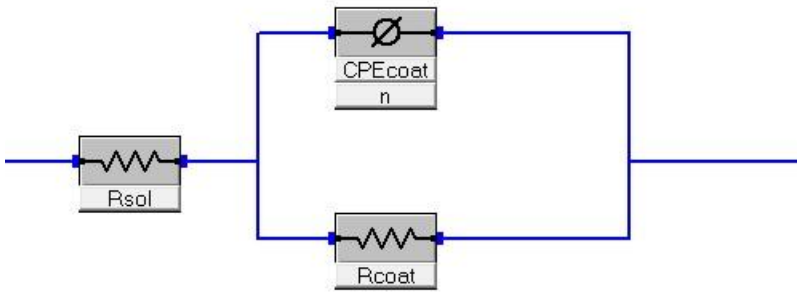

Figure 43. Equivalent circuit used during the measurement of Epoxy Paint reference.

Where $R_{solution}$ is the resistivity of the solution, CPE_{coat} is the constant phase element for the used epoxy coating and R_{coat} is the resistivity of the epoxy coating. For high and low frequencies the $R_{solution}$ and and R_{coat}, are characterized respectively.

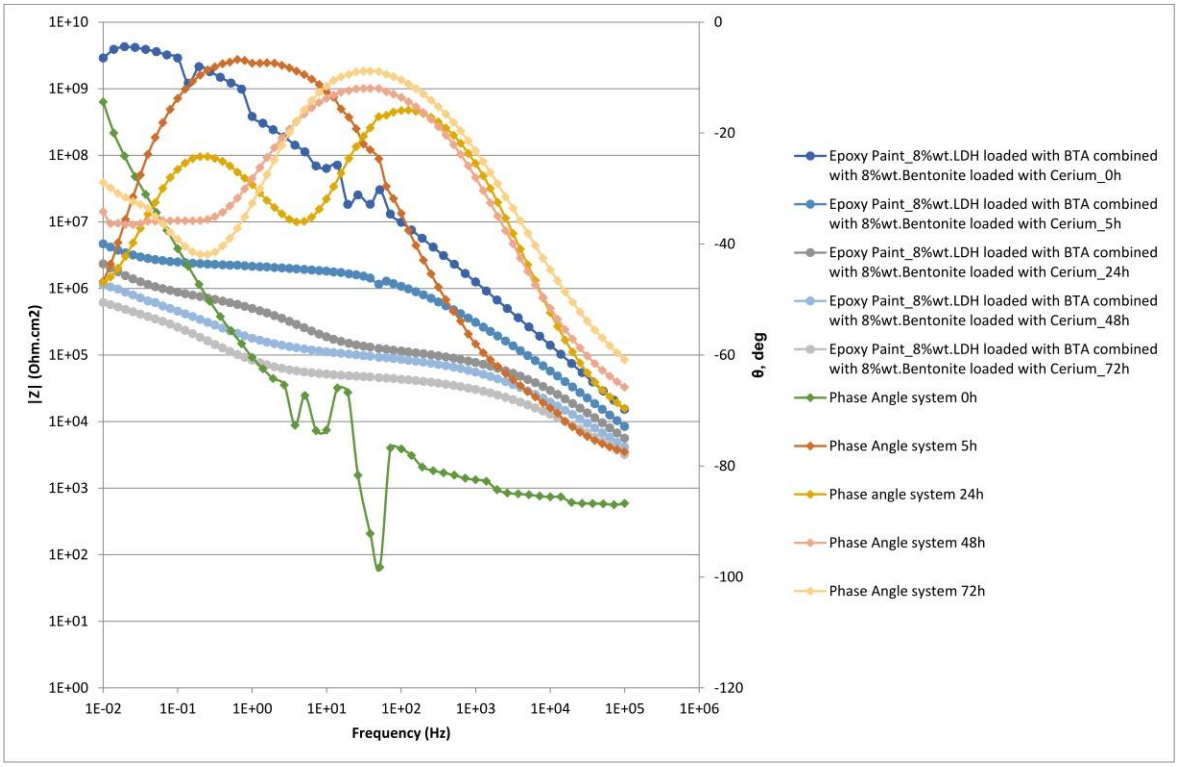

Figure 44. Impedance measurements of the specimens coated with epoxy paint load with 8% wt of LDH loaded with BTA combined with 8% wt of Bentonite loaded with Cerium.

For the coating systems shown in Figure 44 and Figure 45 a different situation appears. Instead of one there are three time constants, one associated to the coating, one related to the pretreatment and the last one to the electrochemical process. Figure 46 shows the equivalent circuit used for these two formulations.

When the two loaded nanocontainers were added, the properties of the coatings changed, the total resistivity drops three decades. It can be explained by the formation of microscratches into the coating in presence of loaded nanocontainers inside. For Figure 42 and Figure 44 the modification of the EIS signal from one coating formulation to another is negligible between 0 hours and 5 hours of immersion and can be interpreted as a deviation during the measurements.

It is evident that the nanocontainers have a huge influence on the quality of the coating.

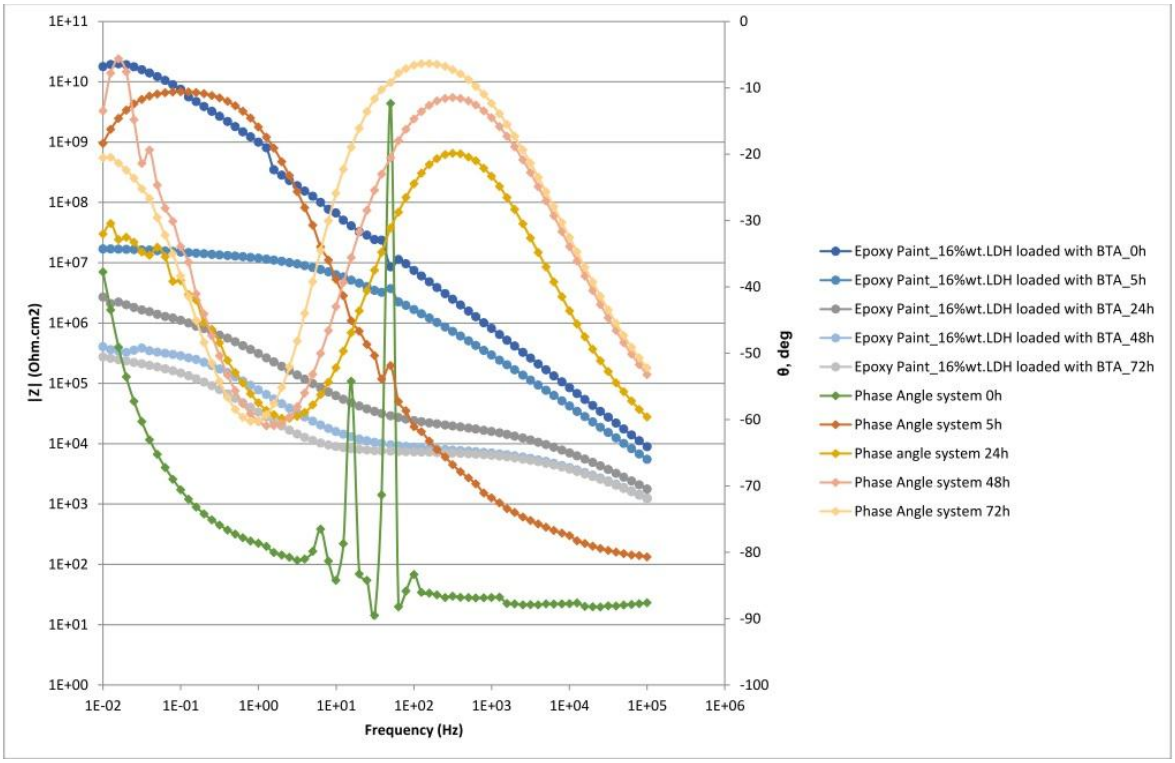

Figure 45. Impedance measurements of the specimens coated with epoxy paint load with 16% wt of LDH.

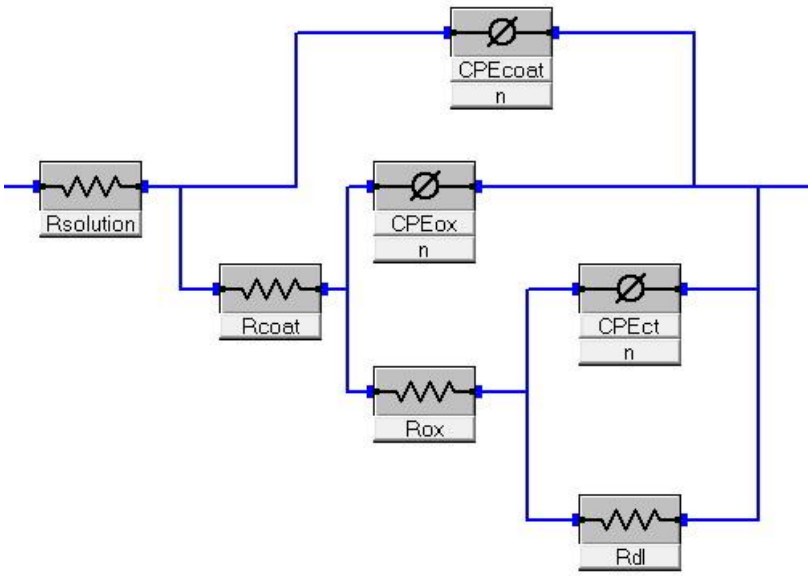

Figure 46. Equivalent circuit used during the measurements.

Where $R_{solution}$ is the resistivity of the solution, CPE_{coat} is the constant phase element for the used epoxy coating, R_{coat} is the resistivity of the epoxy coating, R_{ox} is the resistivity of the oxide layer, CPE_{ox} is the constant phase element for the oxide layer,

CPE_{ct} is the constant phase element for the charge transfer and R_{ox} is.the resistivity of the double layer.

Figure 47 characterizes the different behaviours of the three formulations of epoxy paint at the same time. The system without nanocontainers reveals higher values of resistivity them the other systems. So the divergency between the other two systems is related to the nanocontainers incorporated and the way they can influence the coating.

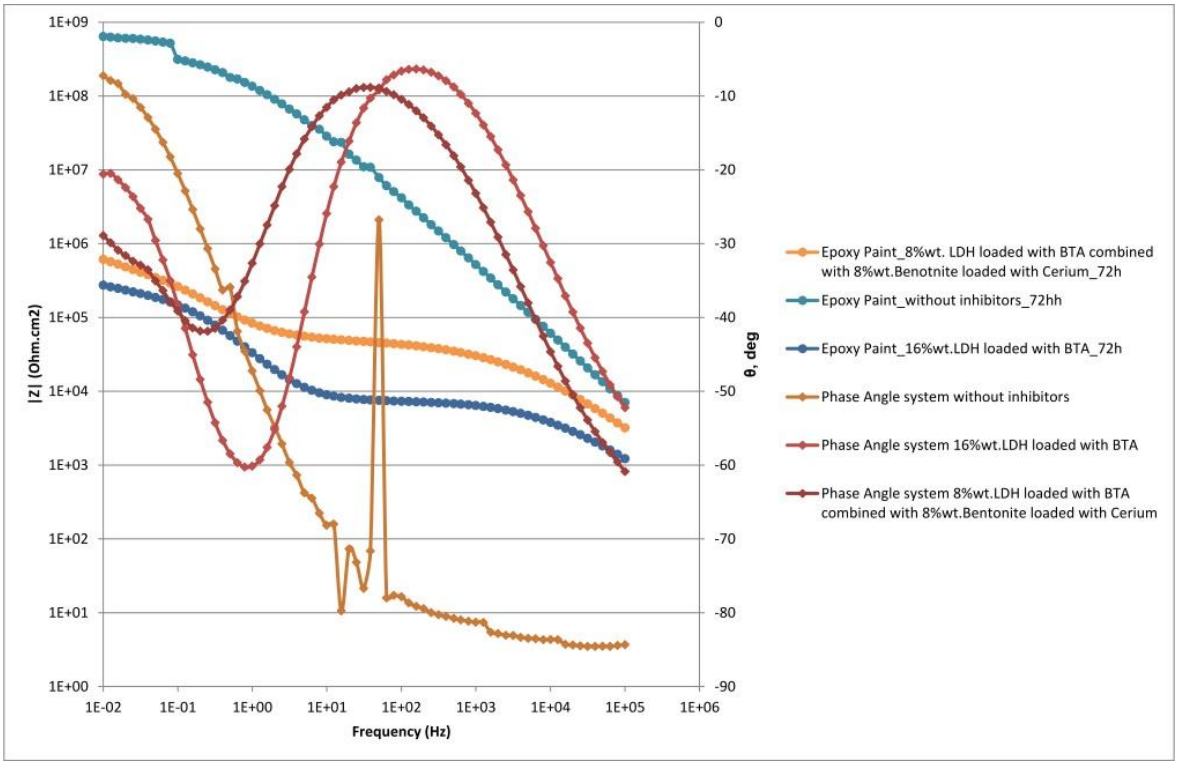

Figure 47. Comparison of EIS results for all formulations of the epoxy system for a selected period of time.

Table 12. Relation between Resistivity and Constante phase from each system.

System	Time (h)	R_{coat} (ohm.cm²)	C_{coat} (S.sᵃ/cm²)	$R_{ox.}$ (ohm.cm²)	$C_{ox.}$ (S.sᵃ/cm²)	R_{ct} (ohm.cm²)	C_{dl} (S.sᵃ/cm²)
Ref.	0	$5{,}07\text{x}10^{10}$	$3{,}01\text{x}10^{-10}$	-	-	-	-
Ref.	24	$8{,}34\text{x}10^{8}$	$8{,}00\text{x}10^{-10}$	-	-	-	-
LDH	0	$2{,}50\text{x}10^{10}$	$2{,}39\text{x}10^{-10}$	-	-	-	-
LDH	24	$1{,}70\text{x}10^{4}$	$2{,}26\text{x}10^{-9}$	$1{,}33\text{x}10^{6}$	$5{,}03\text{x}10^{-7}$	$1{,}05\ \text{x}10^{-3}$	$6{,}53\text{x}10^{-7}$
Mixt.	0	$2{,}63\text{x}10^{9}$	$2{,}52\text{x}10^{-10}$	-	-	-	-
Mixt.	24	$4{,}84\text{x}10^{4}$	$3{,}81\text{x}10^{-10}$	$7{,}31\text{x}10^{4}$	$3{,}12\text{x}10^{-9}$	$6{,}66\text{x}10^{5}$	$2{,}18\text{x}10^{-7}$

5.4.2. Sol-gel coating

Figure 48 to Figure 51 represent the prepared formulations for the sol-gel coating system. They describe the evolution with time for each system.

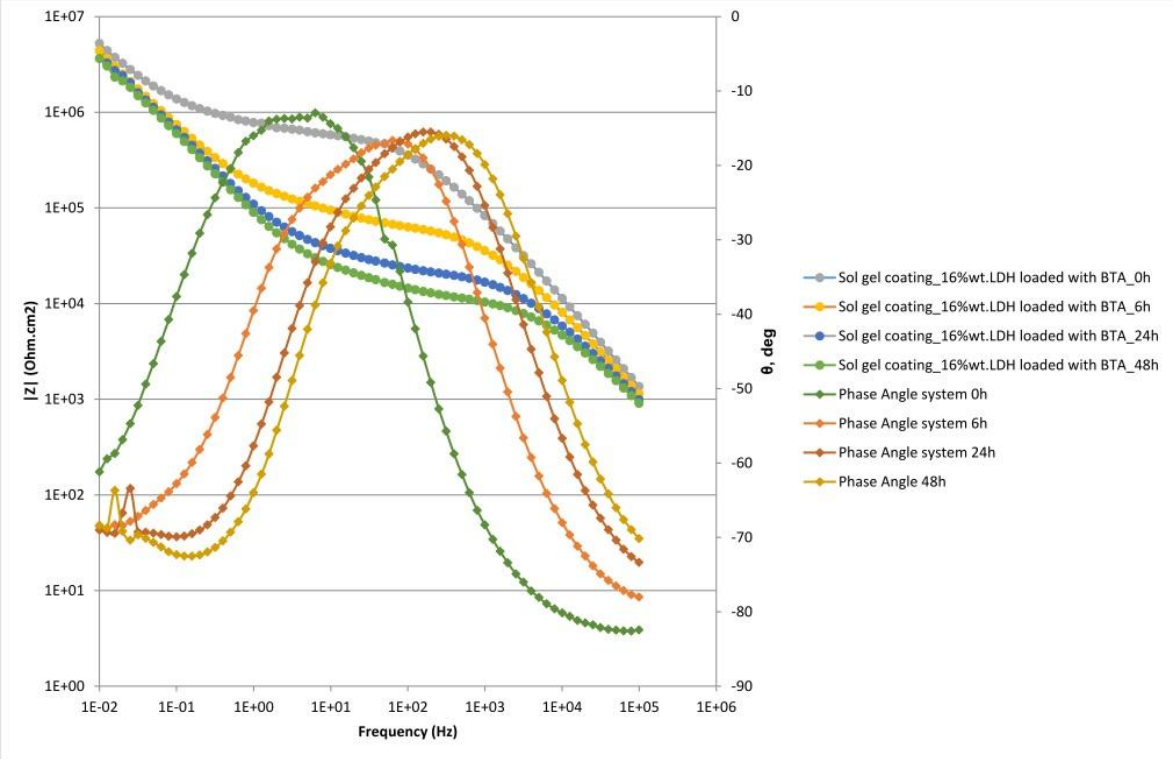

Figure 48. Impedance measurements of the specimens coated with sol-gel load with 16% wt of LDH loaded with BTA.

The equivalent circuit used for this arrangement is shown in Figure 49. It is composed by three time constants: one associated to the coating, one related to the pretreatment and the last one to the oxidation process, which means that the barrier properties from the coating are not the best.

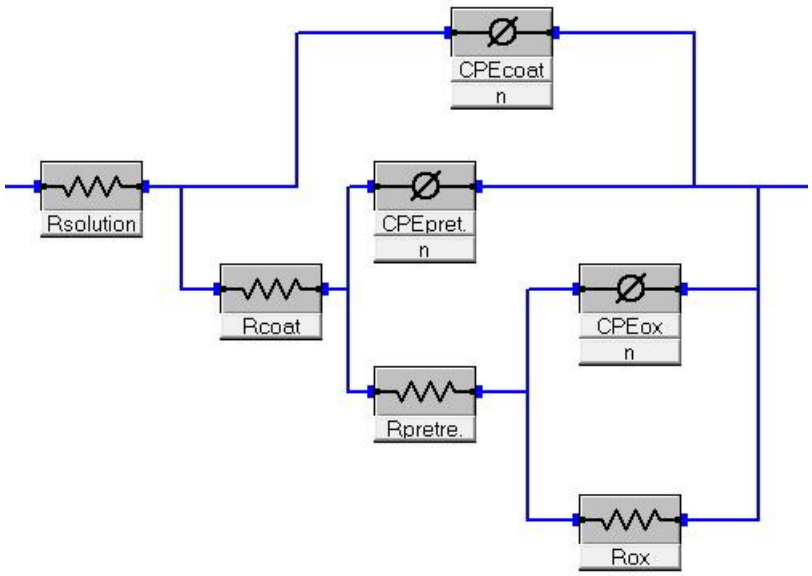

Figure 49. Equivalent circuit used during the measurements.

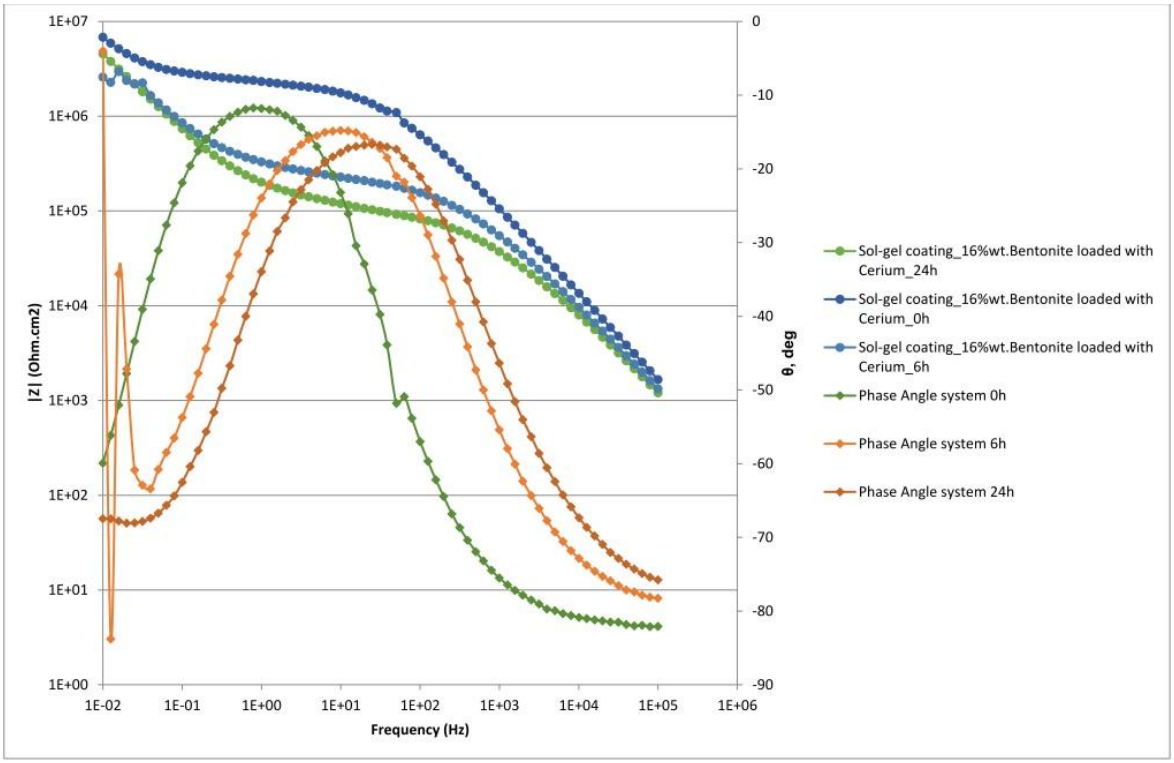

Figure 50. Impedance measurements of the specimens coated with sol-gel load with 16% wt of Bentonite loaded with Cerium.

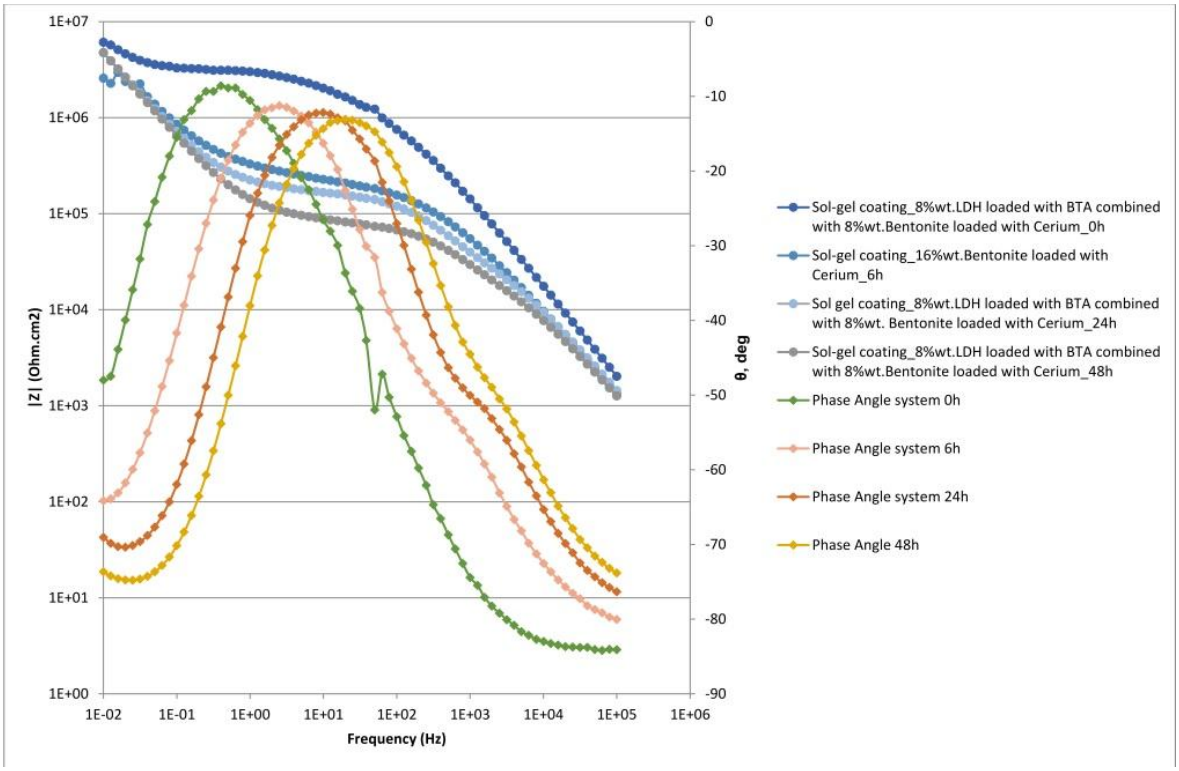

Figure 51. Impedance measurements of the specimens coated with sol-gel with 8% wt of LDH loaded with BTA combined with 8% wt of Bentonite loaded with Cerium.

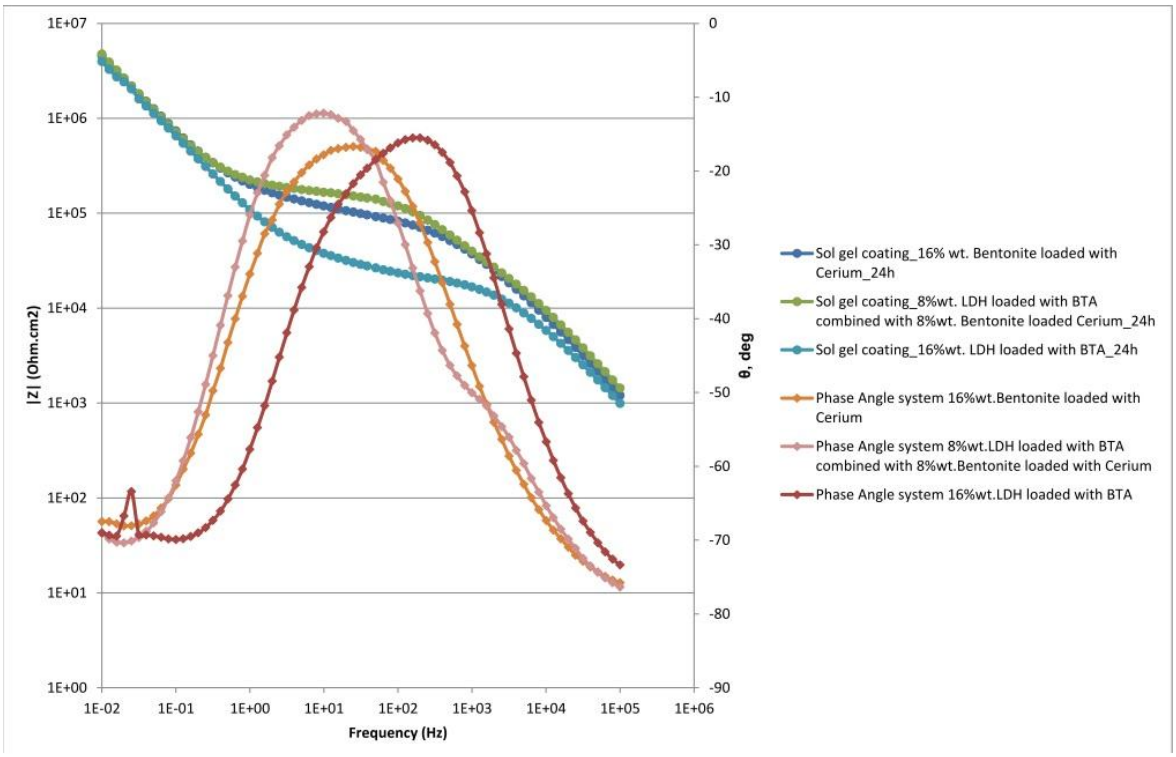

Figure 52. Comparison of EIS results for all the performed formulations of sol-gel formulation for a selected period of time.

Evaluating Figure 52, no big differences between the three systems can be observed. However, the 16%wt LDH loaded with BTA presents a drop for higher frequencies that could be related with the porosity of the coating. During the immersion period in 0.50 M of NaCl an optical inspection was done to each specimen, the only observation were a small amount of air bubbles.

By analysing Figure 48, Figure 50 and Figure 51 it is possible to verify that independently of the formulation the total resistivity of the coating doesn't change. However, from the Figure 47 and Figure 52 it can be derived, that the resistivity of the epoxy coating (10^{10} ohm.cm^2) is significantly higher than the resistivity of sol-gel coating (10^6 ohm.cm^2). Since the coating was performed by a machine with specific parameters for thickness of the coating, these values describe the barrier issues in other words, the barrier properties of the epoxy coating are better than the ones of the sol-gel coating. Therefore the epoxy paint will protect the specimen from corrosion more effectively than the sol-gel. Table 14 shows the sample matrix used for the final tests.

Table 13. Relation between Resistivity and Capacitance from each system.

System	Time (h)	R_{coat} (ohm.cm^2)	C_{coat} (S.s^a/cm^2)	R_{pret} (ohm.cm^2)	C_{pret} (S.s^a/cm^2)	R_{ox} (ohm.cm^2)	C_{ox} (S.s^a/cm^2)
Bent.	0	4,99x10^5	1,37x10^{-9}	1,73x10^6	2,71x10^{-9}	2,01x10^7	2,10x10^{-6}
Bent.	24	3,84x10^4	2,00x10^{-9}	8,04x10^4	1,39x10^{-8}	7,77x10^6	2,39x10^{-6}
LDH	0	2,39x10^5	1,61x10^{-9}	4,41x10^5	5,81x10^{-9}	8,36x10^6	2,19x10^{-6}
LDH	24	1,84x10^4	2,60x10^{-9}	4,17x10^4	3,97x10^{-7}	6,39x10^6	2,14x10^{-6}
Mixt.	0	4,96x10^5	1,02x10^{-9}	1,43x10^6	1,76x10^{-9}	1,33x10^6	3,57x10^{-8}
Mixt.	24	3,06x10^4	1,54x10^{-9}	1,37x10^5	6,50x10^{-9}	1,00x10^7	2,55x10^{-6}

Table 14. Sample matrix with all the systems to be prepared.

Sample number	Surface (mm^2)	Pre-treatment	Coating	LDH %	LDH (g)	Bent. %	Bent. (g)	Paint (g)	Resin (g)	Hard (g)
1	3500	socosurf	EP	0	0	0	0	210	150	60
2	12000	socosurf	EP	0	0	0	0	210	150	60
3	12000	socosurf	EP	0	0	0	0	210	150	60
4	3500	socosurf	EP	0	0	16	33,6	210	150	60
5	12000	socosurf	EP	0	0	16	33,6	210	150	60
6	12000	socosurf	EP	0	0	16	33,6	210	150	60
7	3500	socosurf	EP	8	16,8	8	16,8	210	150	60
8	12000	socosurf	EP	8	16,8	8	16,8	210	150	60
9	12000	socosurf	EP	8	16,8	8	16,8	210	150	60
10	3500	socosurf	EP	16	33,6	0	0	210	150	60
11	12000	socosurf	EP	16	33,6	0	0	210	150	60
12	12000	socosurf	EP	16	33,6	0	0	210	150	60
13	3500	socosurf	SG	0	0	0	0	150	-	-
14	12000	socosurf	SG	0	0	0	0	150	-	-
15	12000	socosurf	SG	0	0	0	0	150	-	-
16	3500	socosurf	SG	0	0	16	24	150	-	-
17	12000	socosurf	SG	0	0	16	24	150	-	-
18	12000	socosurf	SG	0	0	16	24	150	-	-
19	3500	socosurf	SG	0	0	16	24	150	-	-
20	3500	socosurf	SG	8	12	8	12	150	-	-
21	12000	socosurf	SG	8	12	8	12	150	-	-
22	12000	socosurf	SG	8	12	8	12	150	-	-
23	3500	socosurf	SG	16	24	0	0	150	-	-
24	12000	socosurf	SG	16	24	0	0	150	-	-
25	12000	socosurf	SG	16	24	0	0	150	-	-

Chapter 6: Conclusions

6. Conclusions

This work was done in frame of an internshit under industrial environment which allowed me to get in touch with new techniques and equipments. Among the time spent in the company I was able to learn techniques releated with corrosion, coating compatibility and surface treatment such as, salt spray test, drop test, adhesion test, EIS measureaments and plasma treatment.

The main aims for this work were achieved: (1) first aim was to obtain a reproducible assembly through which it would be possible to prove the galvanic effect and the (2) second find a system that would prevent the corrosion and be environmenral friendly at the same time.

The results related to the prove of galvanic effect show that the assembly works, it is reproducible and there is galvanic effect happening.

The analysis of all obtained results allows to conclude that the best system is : 8%wt.LDH loaded with BTA combined with 8%wt.Bentonite loaded with Cerium (Epoxy paint) because of:

- Adhesion and scratch test: Good adhesion, no defects detected, even after 2 weeks of immersion.
- Drop test: lower amount of corrosion products.
- EIS measurements: higher resistivity when compared to the others two systems.
- SST test: All the formulations with nanocontainers presented blisters that can be related with incompatibility between paint and nanocontainers, osmotic exchanges or pH problems.

Chapter 7: Future work

7. Future Work

- Analyse the LDH nanocontainers loaded with BTA perform the characterization from the nanocontainers and also from the inhibitor.
- Improve the dispersion of Bentonites in order to obtain a better coating, especially for the epoxy paint.
- Perform impedance measurements with a higher duration.

Chapter 9: References

8. References

1. Deloitte - **2014 Global Aerospace and Defense Industry outlook. Expect another record year for commercial aerospace and continued declines in defense.** United Stats. [Consulted on 13th of March 2015].Available in WWW: http://www2.deloitte.com/us/en/pages/manufacturing/articles/2014-global-aerospace-and-defense-industry-outlook.html.
2. Capgemini - **The Changing Face of the Aerospace & Defense Industry: Review of key segments and emerging trends**. [Consulted on 20th of March]. Available in WWW: https://www.capgemini.com/resource-file-access/resource/pdf/The Changing Face of the Aerospace Defense Industry.pdf .
3. Heuss, R., Müller, N., Sistern, v. W., Starke, A., & Tschiesner, A. - **Lightweight, heavy impact: How carbon fiber and other lightweight materials will develop across industries and specifically in automotive.** Available in WWW:http://www.mckinsey.com/search.aspx?q=+Lightweight%2C+heavy+impact%3A+How+carbon+fiber+and+other+lightweight+materials+will+develop+across+industries+and+specifically+in+automotive.
4. Masuelli, A. M. - **Fiber Reinforced Polymers - The Technology Applied for Concrete Repair: Introduction of Fiber-Reinforced Polymers - Polymers and Composites: Concepts, Properties and Processes**. InTech, 2013. ISBN: 978-953-51-0938-9.
5. Palani, S. - **Modelling of galvanic corrosion on hybrid structures in aircraft. Aplication to CFRP - AA2024 unclad material combination.** Brussels: University of Brussels, 2013. Master Thesis.
6. V.S.Sastri.- **Green Corrosion Inhibitors**. Ed. John Wiley & Sons,2011.
7. V.S.Sastri. - **Corrosion Inhibitors: Principles and applications**. Ed. John Wiley & Sons, 1998.

8. Bushman, J. B. - **Corrosion and Cathodic Protection Theory**. USA: Bushman & Associates Inc, 2010.
9. Palani, S.; Hack, T.; Peratta, A.; Adey, R.; Baynham, J.; Lohner, H. - Modelling Approach for Galvanic Corrosion Protection of Multimaterial Aircraft Structures. Department of Defence Corrosion conference 2011, La Quinta 31.7–5.8 2011.
10. McCafferty. E. - **Introduction to Corrosion Science**.New York: Springer,2010. 357-402.
11. Aliofkhazraei, M. - **Developments in Corrosion Protection :Corrosion Inhibitors - Principles, Mechanisms and Applications,** Intech,2014. ISBN 978-953-51-1223-5.
12. Yasakau, K. - **Active corrosion protection of AA2024 by sol-gel coatings with corrosion inhibitors**. Aveiro: University of Aveiro, 2011. PhD thesis.
13. Saji.S, V., & Cook, R. **Corrosion protection and control using nanomaterials**, Woodhead Publishing Limited, 2012. ISBN: 978-1-84569-949-9.
14. Tiwari, A., Rawlins, J., Hihara, H., & Lloyd. **Intelligent Coatings For Corrosion Control**. Elsevier , 2015. ISBN: 978-0-12-411467-8.
15. Rivers, V. **Layered Double Hydroxides: Present and Future**, Nova Science Pub. Inc, 2001. ISBN-13: 978-1590330609.
16. Nalawade, P., Aware, B., Kadam, V., & Hirlekar, R.- Layered double Hydroxides: A review. Journal of Scientific & Industrial Research. Vol.28 (2009), p.267-272.
17. Bierwagen, G. P., Twite, R.L. - Review of alternatives to chromate for corrosion protection of aluminium aerospace alloys. Progress in Organic Coatings. Vol. 33, nº2 (1998), p.91-100.
18. Raps, D. - **Development of a self-healing corrosion protection coating system for high strength aluminium alloys.** Düsseldorf: VDI, 2008.Master thesis.
19. Serrano, J. S. - **Surface Modifications of composite materials by atmospheric pressure plasma treatment**.Madrid: University of Juan Carlos,2011. PhD theis.
20. Henniker Plasma – Plasma Tecnhonology: Overview. Warrington [Last update on 7th of July]. Available in WWW:

<URL:http://plasmatreatment.co.uk/henniker-plasma-technology/plasma-treatments/plasma-surface-activation-to-improve-adhesion/composites/.

21. Cottis, R., & Turgoose, S. **Electrochemical Impedance and Noise.**Corrosion Testing Made Easy, B.C. Syrett Editor, 1999.
22. Schneider O and Kelly RG. - Localized coating failure of epoxy-coated aluminium alloy 2024-T3 in 0,5 M NaCl solutions: Correlation between coating degradation, blister formation and local chemistry within blisters. Corrosion Science. Vol.49 ,nº2 (2007),p. 594 – 619.
23. J. Tedim,S. K. Poznyak,A. Kuznetsova, D. Raps, T. Hack, M. L. Zheludkevich,and M. G. S. Ferreira - Enhancement of Active Corrosion Protection via Combination of Inhibitor-Loaded Nanocontainers ACS Appl. Mater. Interfaces. vol.2, nº 5 (2010), pp.1528–1535.
24. Simillion, H. - **Study of the protective effect of corrosion inhibitors in an organic coating on galvanized steel: Nanocontainers for self-healing coatings**. Brussels: Vrije Universiteit Brussel Faculty of Engineering, 2012. Master's thesis.
25. Vieira, Daniel - **Active protective treatments for galvanically coupled AA2024 and CFRP.** Aveiro: University of Aveiro, 2014. Master's thesis.
26. Nabel A. Negm, Mona A. Yousef and Salah M. Tawfik. Impact of Synthesized and Natural Compounds in Corrosion Inhibition of Carbon Steel and Aluminium in Acidic Media.. Corrosion Science. Nº3, 2013.
27. T.L. Metroke, R.L. Parkhill. E.T. Knobbe. Prog. Org. Coat.. Vol. 41. 2001, p. 233.
28. M .L. Zheludkevich, R. Serra, M.F. Montemor, I.M. Miranda Salvado, M.G.S. Ferreira. Corrosion protective properties of nanostructured sol–gel hybrid coatings to AA2024-T3. Surface and Coatings Technology, nº 200, 2006. p.3084- 3094.
29. R.L. Twite, G.P. Bierwagen. Prog. Org. Coat.. Vol.33. 1998, p.91.
30. R.G. Buchheit, H. Guan, S. Mahajanam, F. Wong. Prog. Org. Coat. Vol. 47. 2001, p. 174.
31. E. Almeida, L. Fedrizzi, T.C. Diamantinio. Surf. Coat. Technol. Vol. 105. 1998, p.97.
32. R.L. Twite, G.P. Bierwagen. Prog. Org. Coat. Vol. 33. 1998, p. 91.

33. B.F. Rivera, B.Y. Johnson, M.J. O'Keefe, W.G. Fahrenholtz. Surf. Coat. Technol. Vol. 176. 2004, p. 349.
34. M. Dabala, E. Ramous, M. Magrini, Mater. Corrosão. Vol. 55. 2004, p.381.
35. J.H. Osborne, K.Y. Blohowiak, S.R. Taylor, C. Hunter, G. Bierwagen, B. Carlson, D. Bernard, M.S. Donley. Prog. Org. Coat. Vol. 41. 2001, p. 217.
36. A.E. Hughes, J.D. Gorman, P.R. Miller, B.A. Sexton, P.J.K. Paterson, R.J. Taylor. Surf. Interface Anal. Vol. 36,2004.p. 290
37. D. Hoebbel, M. Nacken, H. Schmidt, J. Sol-Gel Sci. Technol. Vol.19, 2000.p. 305-309.
38. R.-P. Winkler, E. Arpac, H. Schirra, S. Sepeur, I. Wegner, H. Schmidt. Thin Solid Films. Vol.351,1999.p. 209-211,
39. E. Geiter. Universität des Saarlandes (1997). PhD thesis.
40. T. Vogeler, M. Kreuzer, T. Tschudi, F. Simoni. Molecular Crystals & Liquid Crystals, Vol.282,1996.p. 419-428.
41. T. Hübert, A. Shimamura, A. Klyszcz. Mater. Sci.-Poland. Vol.23, nº1 (2005).p.61-68.
42. L.G. Anderson, K.A. Barkac, A.M. Chasser, S.A. Desaw, M.A. Hartman, D.E. Hayes, T.R. Hockswender, K.L. Kuster, R.A. Montague, M. Nakajima, K.G. Olson, J.S. Richardson, R.J. Sadvary, D.A. Simpson, S. Tyebjee, T.F. Wilt, PPG ndustries Ohio, Inc, USA, Chem. Abstr. 134 (2001) p. 164-525.
43. B. Sebastian, Johannes - **Atmosphärenplasma-Beschichtung mit neuartigen Plasmajetquellen zum Korrosionsschutz von Aluminium.** University of Applied Sciences,2007. Master's thesis.
44. Ihde, J., Vissing, K. Oberflächenschutz von Metallen mittels Plasmapolymerisation. Galvanotechnik. ISSN: 016-4232. Vol.98, nº11, p.2794 – 2803.
45. O. Schneider, R.G. Kelly - Localized coating failure of epoxy-coated aluminium alloy 2024-T3 in 0.5 M NaCl solutions: Correlation between coating degradation, blister formation and local chemistry within blisters. Elsevier: Corrosion Science. Vol.49, (2007),p. 594-619.

46. Wegerer M. - **Vorbehandlungsverfahren zur Metallisierung von kohlenstofffaserverstärkten Kunststoffen auf Epoxidharzbasis**. Munich: Technical University of Munich, 2015. Master's thesis.
47. N.Encinas, BR.Oakley, M.A. Belcher, K.Y. Blohowiak, R.G. Dillingham, J. Abenojar, M.A. Martínez. Surface modification of aircraft used composites for adhesive bonding. Elsevier: International Journal of Adhesion & Adhesives. nº 50, 2014. p.157 – 163.
48. L. Shao-Rong, Z. Hai-Liang, Z. Cai-Xian, W. Xia-Yu. Preparation and characterization of epoxy – silica hybrid materials by the sol-gel process. Journal of materials science. nº 40, 2005. p. 1079 – 1085.
49. L. Pinggui, S. Jiangxuan, H. Lihua, L.Xingquan, D. Heyan, L. Qifang. Alkoxysilane ffunctionalized polycaprolactone/polysiloxane modified epoxy resin through sol-gel process. European Polymer Journal. nº 44, 2008. p. 940 – 951.

Estes anexos só estão disponíveis para consulta através do CD-ROM.
Queira por favor dirigir-se ao balcão de atendimento da Biblioteca.

Serviços de Biblioteca, Informação Documental e Museologia
Universidade de Aveiro